In silico and *In vitro* evaluation of the anti-virulance potential of patuletin, a natural methoxyflavone, against *Pseudomonas aeruginosa* (#89813)

First submission

Guidance from your Editor

Please submit by **19 Oct 2023** for the benefit of the authors (and your token reward) .

Structure and Criteria
Please read the 'Structure and Criteria' page for general guidance.

Author notes
Have you read the author notes on the guidance page?

Raw data check
Review the raw data.

Image check
Check that figures and images have not been inappropriately manipulated.

If this article is published your review will be made public. You can choose whether to sign your review. If uploading a PDF please remove any identifiable information (if you want to remain anonymous).

Files
Download and review all files from the materials page.

18 Figure file(s)
1 Raw data file(s)

Structure your review

The review form is divided into 5 sections. Please consider these when composing your review:

1. **BASIC REPORTING**
2. **EXPERIMENTAL DESIGN**
3. **VALIDITY OF THE FINDINGS**
4. General comments
5. Confidential notes to the editor

You can also annotate this PDF and upload it as part of your review

When ready submit online.

Editorial Criteria

Use these criteria points to structure your review. The full detailed editorial criteria is on your guidance page.

BASIC REPORTING

- Clear, unambiguous, professional English language used throughout.
- Intro & background to show context. Literature well referenced & relevant.
- Structure conforms to PeerJ standards, discipline norm, or improved for clarity.
- Figures are relevant, high quality, well labelled & described.
- Raw data supplied (see PeerJ policy).

EXPERIMENTAL DESIGN

- Original primary research within Scope of the journal.
- Research question well defined, relevant & meaningful. It is stated how the research fills an identified knowledge gap.
- Rigorous investigation performed to a high technical & ethical standard.
- Methods described with sufficient detail & information to replicate.

VALIDITY OF THE FINDINGS

- Impact and novelty not assessed. *Meaningful* replication encouraged where rationale & benefit to literature is clearly stated.
- All underlying data have been provided; they are robust, statistically sound, & controlled.
- Conclusions are well stated, linked to original research question & limited to supporting results.

Standout reviewing tips

The best reviewers use these techniques

Tip	*Example*
Support criticisms with evidence from the text or from other sources	*Smith et al (J of Methodology, 2005, V3, pp 123) have shown that the analysis you use in Lines 241-250 is not the most appropriate for this situation. Please explain why you used this method.*
Give specific suggestions on how to improve the manuscript	*Your introduction needs more detail. I suggest that you improve the description at lines 57- 86 to provide more justification for your study (specifically, you should expand upon the knowledge gap being filled).*
Comment on language and grammar issues	*The English language should be improved to ensure that an international audience can clearly understand your text. Some examples where the language could be improved include lines 23, 77, 121, 128 – the current phrasing makes comprehension difficult. I suggest you have a colleague who is proficient in English and familiar with the subject matter review your manuscript, or contact a professional editing service.*
Organize by importance of the issues, and number your points	*1. Your most important issue* *2. The next most important item* *3. …* *4. The least important points*
Please provide constructive criticism, and avoid personal opinions	*I thank you for providing the raw data, however your supplemental files need more descriptive metadata identifiers to be useful to future readers. Although your results are compelling, the data analysis should be improved in the following ways: AA, BB, CC*
Comment on strengths (as well as weaknesses) of the manuscript	*I commend the authors for their extensive data set, compiled over many years of detailed fieldwork. In addition, the manuscript is clearly written in professional, unambiguous language. If there is a weakness, it is in the statistical analysis (as I have noted above) which should be improved upon before Acceptance.*

In silico and *In vitro* evaluation of the anti-virulance potential of patuletin, a natural methoxyflavone, against *Pseudomonas aeruginosa*

Ahmed Metwaly [Corresp., 1, 2], **Moustafa Saleh** [3], **Aisha Alsfouk** [4], **Ibrahim ibrahim** [5], **Muhamad Abd-Elraouf** [1], **Eslam Elkaeed** [6], **Hazem Elkady** [1], **ibrahim eissa** [1]

[1] Al-Azhar University, Cairo, --- Select One ---, Egypt

[2] City of Scientific Research and Technological Applications (SRTA-City), Biopharmaceutical Products Research Department, Genetic Engineering and Biotechnology Research Institute,, Alexandria, Egypt

[3] Port Said University, Port Said, Egypt

[4] Princess Nourah bint Abdulrahman University, Riyadh, Saudi Arabia

[5] cairo university, Giza, Egypt

[6] AlMaarefa University, Riyadh, Saudi Arabia

Corresponding Author: Ahmed Metwaly
Email address: ametwaly@azhar.edu.eg

This study aimed to investigate the potential of Patuletin, a rare natural flavonoid, as a virulence and LasR inhibitor against *Pseudomonas aeruginosa*. Molecular docking revealed that Patuletin strongly bound to the active pocket of LasR, with a high affinity value of -20.96 kcal/mol. Further molecular dynamics simulations, MM-GPSA, PLIP, and essential dynamics analyses confirmed the stability of the Patuletin-LasR complex, and no significant structural changes were observed in the LasR protein upon binding. Key amino acids involved in binding were identified, along with a free energy value of -26.9 kcal/mol. *In vitro* assays were performed to assess Patuletin's effects on *Pseudomonas aeruginosa*. At a sub-inhibitory concentration (1/4 MIC), Patuletin significantly reduced biofilm formation by 48% and 42%, decreased pyocyanin production by 24% and 14%, and decreased proteolytic activities by 42% and 20% in *Pseudomonas aeruginosa* isolate ATCC 27853 (PA27853) and *Pseudomonas aeruginosa* clinical isolate (PA1). Overall, this study demonstrated that Patuletin effectively inhibited LasR activity *in silico* and attenuated virulence factors *in vitro*, including biofilm formation, pyocyanin production, and proteolytic activity. These findings suggest that Patuletin holds promise as a potential therapeutic agent in combination with antibiotics to combat antibiotic-tolerant P. aeruginosa infections.

In silico and *in vitro* evaluation of the anti-virulance potential of Patuletin, a natural methoxyflavone, against *Pseudomonas aeruginosa*

Ahmed M. Metwaly[a,b], Moustafa M. Saleh[c]*, Aisha A. Alsfouk[d], Ibrahim M. Ibrahim[e], Muhamad Abd-Elraouf[a] , Eslam B. Elkaeed[f], Hazem Elkady[g], Ibrahim H. Eissa[g]*

[a] Pharmacognosy and Medicinal Plants Department, Faculty of Pharmacy (Boys), Al-Azhar University, Cairo 11884, Egypt. ametwaly@azhar.edu.eg; mhmraouf@azhar.edu.eg

[b] Biopharmaceutical Products Research Department, Genetic Engineering and Biotechnology Research Institute, City of Scientific Research and Technological Applications (SRTA-City), Alexandria, Egypt.

[c] Microbiology and Immunology Department, Faculty of Pharmacy, Port Said University, Port Said, Egypt. mostafa.mohamed@pharm.psu.edu.eg

[d] Department of Pharmaceutical Sciences, College of Pharmacy, Princess Nourah bint Abdulrahman University, P.O. Box 84428, Riyadh 11671, Saudi Arabia aaalsfouk@pnu.edu.sa;

[e] Biophysics Department, Faculty of Science, Cairo University. Giza 12613, Egypt. ibrahim_mohamed@cu.edu.eg

[f] Department of Pharmaceutical Sciences, College of Pharmacy, AlMaarefa University, Riyadh 13713, Saudi Arabia. ekaeed@um.edu.sa

[g] Pharmaceutical Medicinal Chemistry & Drug Design Department, Faculty of Pharmacy (Boys), Al-Azhar University, Cairo11884, Egypt. hazemelkady@azhar.edu.eg ibrahimeissa@azhar.edu.eg

Corresponding authors: Moustafa M. Saleh and Ibrahim H. Eissa

Abstract

This study aimed to investigate the potential of Patuletin, a rare natural flavonoid, as a virulence and LasR inhibitor against *Pseudomonas aeruginosa*. Molecular docking revealed that Patuletin strongly bound to the active pocket of LasR, with a high affinity value of -20.96 kcal/mol. Further molecular dynamics simulations, MM-GPSA, PLIP, and essential dynamics analyses confirmed the stability of the Patuletin-LasR complex, and no significant structural changes were observed in the LasR protein upon binding. Key amino acids involved in binding were identified, along with a free energy value of -26.9 kcal/mol.

In vitro assays were performed to assess Patuletin's effects on *Pseudomonas aeruginosa*. At a sub-inhibitory concentration (1/4 MIC), Patuletin significantly reduced biofilm formation by 48% and 42%, decreased pyocyanin production by 24% and 14%, and decreased proteolytic activities by 42% and 20% in *Pseudomonas aeruginosa* isolate ATCC 27853 (PA27853) and *Pseudomonas aeruginosa* clinical isolate (PA1).

Overall, this study demonstrated that Patuletin effectively inhibited LasR activity *in silico* and attenuated virulence factors *in vitro*, including biofilm formation, pyocyanin production, and proteolytic activity. These findings suggest that Patuletin holds promise as a potential therapeutic agent in combination with antibiotics to combat antibiotic-tolerant P. aeruginosa infections.

Keywords: Patuletin; *P. aeruginosa*; LasR; MD simulations; ED; Anti-Virulance; Biofilm; Pyocyanin; Proteases

1. Introduction

Pseudomonas aeruginosa (*P. aeruginosa*) is a versatile and opportunistic Gram-negative bacterium classified within the *Pseudomonadaceae* family [1]. *P. aeruginosa* demonstrates remarkable adaptability and can thrive in diverse environments, such as soil, water, and healthcare settings [2]. Additionally, *P. aeruginosa* possesses an array of virulence factors that contribute to its pathogenicity. It produces various toxins, including pyocyanin, which can kill other bacteria competing *P. aeruginosa*, damage host cells and impair immune responses [3]. *P. aeruginosa* also produces proteases that lies in their capacity to cleave essential protein-based components within the host cells allows them to disrupt crucial cellular processes and potentially impair immune defenses enhancing the bacterium's ability to thrive and establish infections within the host [4, 5]. *P. aeruginosa* also can produce biofilms, which provide protection against host defenses as well as antibiotics [6]. As a human pathogen, *P. aeruginosa* is associated with various infections, including pneumonia, urinary tract, and bloodstream infections. *P. aeruginosa* poses a significant risk, particularly to individuals with compromised immune systems or underlying severe health conditions [7].

The field of computational drug discovery utilizes computational techniques, algorithms, and modeling to assist in the exploration of novel drugs or the repurposing of a known one [8]. It employs computer programs and simulations to forecast and examine the interactions between small molecules, which serve as potential drug candidates, and target biomolecules like proteins [9]. The integration of computational drug discovery into drug design has become highly relevant, playing a crucial role in the practical implementation of predictive modeling within pharmaceutical research and development. Our team utilized computational drug discovery methodologies in various aspects, including molecular docking [10], molecular design, toxicity [11], ADMET [12], DFT [13, 14], structural similarity [15], MD [16], and pharmacophore [17] evaluation.

In *P. aeruginosa*, the LasR protein is a key component that acts as a transcription factor that regulates the expression of numerous genes involved in virulence factors production, biofilm formation, and other important physiological processes [18]. LasR is a receptor protein that binds to small signaling molecules called N-acyl homoserine lactones [19]. When the concentration of

these molecules reaches a certain threshold, LasR undergoes a conformational change, enabling it to bind to specific DNA sequences and activate the expression of target genes [20]. This activation leads to the production of various virulence factors such as pyocyanin, biofilm-related enzymes, and other molecules that contribute to *P. aeruginosa*'s pathogenicity [21].

Throughout history, nature has been the source of necessities for humans, including medicine, sustenance, and beauty products [22, 23]. From 1981 to 2014, natural products accounted for nearly one-third of all newly approved drugs by the FDA, and this trend has persisted for many years [24, 25]. Patuletin, an uncommon methoxyflavone, was initially discovered in *Tagetes patula* in 1941 [26]. Since then, it has been found in only a few other plants such as *Urtica urens* [27] and *Eriocaulon* sp. [28]. Despite its scarcity, some scientific studies have investigated and confirmed the antimicrobial potential of Patuletin [29, 30].

Flavonoids have demonstrated potent inhibition against various virulence factors in *P. aeruginosa*, including pyocyanin, protease production and biofilm formation [31]. Numerous flavonoids, that are very near in structure to Patuletin (Figure 1), interacted with and inhibited the LasR protein. For instance, Hispidulin [32], Quercetin [33, 34], Luteolin [35], Naringenin [36], Taxifolin [37] and Catechin [38] exhibited high inhibition potentialities against the LasR protein offering promising hope for the development of novel therapeutic strategies to combat infections caused by *P. aeruginosa*. The inhibition of LasR activity disrupts the quorum sensing system of *P. aeruginosa*, interfering with its ability to coordinate and carry out virulent activities leading to decrease virulence factors production [39]. Accordingly, targeting the LasR's inhibition offers a potential strategy for controlling *P. aeruginosa* infections and mitigating the associated virulence and biofilm formation.

In this research, the great structural similarities between Patuletin and **TY4**, the cocrystallized ligand and several reported flavonoid inhibitors of LasR protein (**Figure 1**) inspired us to examine the *in silico* and *in vitro* potential of Patuletin against LasR protein and *P. aeruginosa* virulence factors.

Figure 1. Chemical structures of Patuletin, cocrystallized ligand (**TY4**) and reported flavonoid inhibitors of LasR protein

2. Materials and methods

2.1. Docking studies

Was operated for Patuletin against LasR protein by MOE2014 software [40]. The supplementary section offers further elaboration contributing additional and specific information.

2.2. M D simulations

Was operated for the Patuletin-LasR complex by the CHARMM-GUI web server [41] and GROMACS 2021. The supplementary section offers further elaboration contributing additional and specific information [42, 43].

2.3. MM-GBSA

Was operated for the Patuletin-LasR complex by the Gmx_MMPBSA package [44, 45]. The supplementary section offers further elaboration contributing additional and specific information.

2.4. ED analysis

PCA analysis was employed to investigate the dynamic motion of alpha carbons located in the amino acid sequence spanning [46]. The supplementary section offers further elaboration contributing additional and specific information.

2.5. Bi-dimensional assays

To compare frames within the reduced subspace, we merged, aligned, created a new C matrix, and plotted the projections [47]. The supplementary section offers further elaboration contributing additional and specific information.

2.6. Active compound

Patuletin was isolated from Tagetes patula as described before [48].

2.7. Bacterial isolates

In the current study, one clinical *P. aeruginosa* isolate (PA1) and a standard *P. aeruginosa* isolate ATCC27853 (PA27853) were used. The supplementary section offers further elaboration contributing additional and specific information.

2.7. Determination of the minimum inhibitory concentration (MIC) of Patuletin

Using the broth microdilution technique following Clinical and Laboratory Standards Institute (CLSI) procedures [49], the MIC of Patuletin was assessed. The supplementary section offers further elaboration contributing additional and specific information.

2.8. Evaluation of Patuletin impact on virulence factors production in *P. aeruginosa*

2.8.1. *Biofilm inhibition assay*

According to the reported procedures [50], the ability of the tested isolates to generate biofilms was evaluated. The supplementary section offers further elaboration contributing additional and specific information.

2.8.2. *Pyocyanin inhibition assay*

Pyocyanin estimation was carried out following the reported [51] procedures. The supplementary section offers further elaboration contributing additional and specific information.

2.8.3. *Proteases inhibition assay*

According to the reported procedures [52], the modified skim milk technique was used to assess the Patuletin ability to suppress the production of proteases. The supplementary section offers further elaboration contributing additional and specific information.

2.9. Statistical analysis

The GraphPad Prism 7 software package was used to analyze the data for the current study. The supplementary section offers further elaboration contributing additional and specific information.

3. Results and disscusions

Computational (*In silico*) Studies

3.1. Molecular docking

The molecular interaction of Patuletin with the LasR protein was accomplished by a docking study using the Molecular Operating Environment (MOE, 2019) software. The 3D structure of *P. aeruginosa* LasR was downloaded from the Protein Data Bank (http://www.rcsb.org/pdb/) with the code: 3JPU (Resolution: 2.30 Å). At first, the co-crystallized ligand (**TY4**) was docked in the active site to validate the docking procedure. The superimposition of the docked and co-crystallized ligands produced an RMSD value of 0.40 Å that advocates the correctness of the docking job (**Figure 2**).

Figure 2. Superimposition of the docked pose (blue) and the co-crystallized one (pink) inside of the active site of LasR protein with an RMSD value 0.40 Å.

Regarding the binding mode of the co-crystallized ligand (**TY4**) against the active pocket of the LasR protein, it exhibited a binding score of -27.75 kcal/mol. Its binding pattern showed two hydrogen bonds, one electrostatic interaction, and twenty-five hydrophobic interactions. The 2-chlorobenzamidomethyl and 2,4-dichlorobenzoate arms occupied the first sub-pocket of the active site to form three hydrogen bonds with Asp73, Tyr56, and Trp60 besides a network of pi-pi and pi-alkyl bonds with Ala105, Leu110, Phe101, Val76, Tyr47, Ala127, Cys79, Gly126, Leu125, Ala50, and Leu40. In addition, the 4-bromo-6-methylphenyl moiety was inserted in the second pocket forming six hydrophobic interactions with Tyr64, Arg61, and Leu36 (**Figure 3**).

Figure 3. A) 3D interaction of the co-crystallized ligand (**TY4**) in the active site of the LasR protein. **B)** 2D interaction of **TY4** in the active site of LasR protein. **C)** Mapping surface showing **TY4** occupying the active site of LasR protein.

The top docking pose of Patuletin showed that it occupied the active pocket of the LasR protein with an affinity value of -20.96 kcal/mol. The binding pattern revealed six hydrogen bonds, eight hydrophobic interactions, and two electrostatic interactions. In detail, the 3,5,7-trihydroxy-6-methoxy-4H-chromen-4-one moiety occupied the first sub-pocket of the active site to form four hydrogen bonds with Ser129, Thr115, and Thr75. Also, the same moiety formed four hydrophobic interactions with Tyr56, Tyr64, and Leu36 besides two electrostatic interactions with Asp73. On the other hand, the pyrocatechol moiety occupied the second pocket forming two hydrogen

bonding interactions with Asp65 and Arg61 and four hydrophobic interactions with Arg61, Leu36, Ile52, and Leu36 (**Figure 4**).

Figure 4. A) 3D interaction of Patuletin in the active site of LasR protein. **B)** 2D interaction of Patuletin in the active site of LasR protein. **C)** Mapping surface showing Patuletin occupying the active site of LasR protein.

3.2. MD simulations

Molecular dynamics (MD) simulations offer a reliable computational technique to examine and understand protein dynamics and atomic-level structural changes [53]. Through precise modeling of the movements and interactions of atoms within a protein, MD simulations allow the study of conformational variations that arise during the binding of ligands. These simulations yield significant information about the energetic and dynamic characteristics of proteins, offering insights into the mechanisms behind ligand recognition and the structural modifications induced by binding [54].

Root-mean-square-deviation (RMSD) values for apo LasR protein (blue line) are lower on average than those for holo LasR protein (red line) during the first 40 ns, with a difference of 0.5 Å. In the subsequent 20 ns, both the apo and holo LasR proteins exhibit a small rise. At the end of the final 40 ns, the two proteins exhibit an average of roughly 1.5 Å. (**Figure 5**.A). In the first 60 ns, the root-mean-square-deviation (RMSD) of the Plateulin varies in value before settling at an average of 6.5 Å for the last 40 ns (**Figure 5**.B). **Figure 5**.B's inset explains why there is such a huge RMSD between the first frame and subsequent frames after the first 60 ns. Plateulin reorients itself with respect to the LasR protein while staying in the binding pocket. **Figure 5**.C shows that the average radius of gyration for both the apo and holo LasR protein is around 15.5 Å. Similar trends may be seen in the SASA values, with both apo and holo LasR proteins averaging approximately 9650 $Å^2$. According to **Figure 5**.E, the average number of H-bonds in the apo and holo systems is quite similar (39 bonds). In conclusion, neither LasR protein is undergoing any major structural changes upon binding with Plateulin. Furthermore, the C-alpha atomic oscillations of the two systems follow essentially the same trend (**Figure 5**.F). As can be seen in **Figure 5**.G, the values follow a similar trend to that of Plateulin's RMSD. It varies for the first 60 ns before settling at 9.2 Å in the last 40 ns.

Figure 5. A) RMSD values from the trajectory for the LasR protein in apo (blue line) and holo forms (red line), B) shows Plateulin RMSD values, C) radius of gyration for the protein in apo and holo forms, D) SASA for the holo forms, E) change in the number of hydrogen bonds for the protein in apo and holo forms, F) RMSF for the LasR protein in apo and holo forms, G) distance from the center of mass of Plateulin compound and LasR protein.

3.3. MM-GBSA

The key components of the computed binding free energy of the Plateulin-LasR complex using the MM-GBSA approach are shown in Figure 6. A binding energy of -26.9 kcal/mol for Plateulin suggests a promising binding strength. Binding stability seems to be determined more slightly by Van der Waals interactions than electrostatic ones (-35.18 Kcal/Mol vs. -28.75 Kcal/Mol). Several amino acids within 1 nm of Plateulin were used in an estimate of their contribution using decomposition analysis (Figure 7). Leu36 (-1.57 Kcal/Mol), Tyr47 (-4 Kcal/Mol), Tyr67 (-1.9 Kcal/Mol), Asp65 (-1.15 Kcal/Mol), and Ala70 (-1.11 Kcal/Mol) are the amino acids with a binding energy of less than -1 Kcal/Mol.

Figure 6. Energetic components of MM-GBSA and their values. Bars represent the standard deviations.

Figure 7. Binding free energy decomposition of the Plateulin -LasR complex.

3.4. Protein-Ligand Interaction Fingerprint (ProLIF) Study~~ProLIF and PLIP studies~~

~~Based on the data from t~~The ~~ProLIF library studies~~ ~~determine the evolution of different interactions formed between the ligand and amino acids within the pre-defined cutoff~~, ~~ProLIF is an essential method utilized in computer-aided drug design, molecular docking, and MD investigations. It plays a crucial role in thoroughly examining and characterizing the interactions between proteins and ligands. The ProLIF approach involves generating interaction fingerprints, which are distinct patterns resulting from the interplay between a protein and a ligand. These~~

~~fingerprints are pivotal for quantifying both the strength and nature of binding interactions. ProLIF enables the quantification of various interaction types, including important categories like hydrogen bonds, hydrophobic contacts, and other non-covalent associations [55]. Additionally, in the context of MD simulations, ProLIF serves as a valuable tool for monitoring the dynamic behavior of protein-ligand complexes over extended timeframes. It provides valuable insights into how interactions between the protein and ligand evolve throughout the simulation, thus enhancing our comprehension of complex stability and binding affinity [56]~~. Based on the data from the ProLIF library, we know that three amino acids have a 79-percent-or-higher interaction rate. The three most common interacting amino acids are Leu36 (97%), Tyr47 (86.6%), and Tyr64 (99.6% hydrophobic, 79% pi stacking) (Figure 8).

Figure 8. The amino acids, the types of interactions with Plateulin, and their occurrence during the whole simulation time using the ProLIF Python library.

3.5. Protein-Ligand Interaction Profiles (PLIP) study

~~PLIP, a prominent bioinformatics tool, plays a central role in dissecting and illustrating interactions occurring within molecular assemblies that involve both a protein and a ligand. This computational approach provides invaluable insights into the binding interactions and non-covalent connections established between the ligand and the protein. These revelations unveil the intricate molecular mechanisms that govern ligand-receptor interactions [57]. Given its paramount relevance across fields such as drug discovery, computational biology, and structural bioinformatics, PLIP has gained widespread adoption for the comprehensive analysis of protein-ligand complexes and their interplay. When integrated with other computational techniques, such as molecular docking, MD simulations, and free energy calculations, PLIP facilitates a profound understanding of ligand-protein interactions [58]. As a result, PLIP stands as a crucial method in the realm of rational drug design. PLIP was employed to extract the 3D binding interactions in .pse file format from the representative frames obtained through clustering [59]~~ The 3D binding interactions were extracted using PLIP from the clustering-derived representative frames as .pse files. The determination of the number of clusters was automated using the elbow method, resulting in a total of four clusters (Figure 9), as explained in the methods section. This approach facilitated the identification of distinct groups or patterns of Plateulin -LasR interactions within the trajectory data. Once the clusters were established, the subsequent step involved selecting a representative frame from each cluster. These frames served as snapshots or examples capturing the overall behavior exhibited by the Plateulin -LasR complex within each cluster. They succinctly represented the unique characteristics and dynamics observed within their respective groups. To further examine the interactions within the Plateulin -LasR complex, the PLIP webserver was employed for each representative frame. The PLIP webserver is a valuable tool used for the identification and analysis of protein-ligand interactions. By utilizing this resource, we gained insights into the number and types of interactions occurring within the Plateulin -LasR complex in each specific cluster. This analysis provided valuable information regarding the binding patterns, molecular interactions, and potential functional implications of Plateulin within the LasR protein.

Figure 9. The four clusters representative obtained from TTClust and their 3D interactions with Plateulin. Grey dashed lines: hydrophobic interactions, blue solid lines: H-bonds, green dashed lines: pi-stacking, orange sticks: Plateulin, blue sticks: amino acids of the LasR protein.

To assess the enduring stability of the binding modes within the Plateulin-LasR complex, we embarked on a comprehensive analysis that spanned a simulation process lasting 100 nanoseconds, utilizing data extracted from both ProLIF and PLIP to determine the most essential thee interactions and depict the key distances between Patuletin's atoms and the LasR's active site through these interactions. The results of this analysis are visually depicted in Figure 10 illustrating the fluctuations in the distances characterizing these key interactions over the course of the simulation. Specifically, the distance between Leu36 and atom C13 within Plateulin is denoted by the blue line. The red line tracks the variations in distance between Leu36 and atom C6 within Plateulin. Lastly, the green line elucidates the dynamic changes in the distance between Tyr64 and atom C13 within Plateulin. This in-depth examination of these interactions provides valuable insights into the structural dynamics and stability of the Plateulin-LasR complex during the simulation, shedding light on the pivotal roles these molecular interactions play in the binding process.

Figure 10. A) Show the change in the distances of three key interactions (as obtained from ProLIF and PLIP). Blue line: shows the distance between Leu36 and atom C13 in Plateulin, Red Line: shows the distance between Leu36 and atom C6 in Plateulin, and Green line: shows the distance between Tyr64 and atom C13 in Plateulin. B) Shows the atom names of Plateulin

3.5. ~~ED,~~ Principal Component Analysis (PCA)

We employed principal component analysis (PCA) to locate the coordinated actions. As noted in the methodology section, we used the scree plot, the eigenvector distribution, and the variance maintained with additional eigenvectors (cumulative total) to determine the size of the reduced subspace. At the second PC, the slope of the scree plot noticeably flattens out. Alone, the first eigenvector accounted for about 63% of the entire variance, whereas the first three eigenvectors together accounted for approximately 74.66% of the total variance (Figure 11). It was shown that the first five PCs did not have a normal distribution (Figure 12). As a whole, we represented the essential subspace using the top three eigenvectors.

Figure 11. ~~shows~~ the change in the eigenvalues with increasing the eigenvectors (blue line). In addition, the cumulative variance retained in the eigenvectors is shown (red line).

Figure 12. The distribution of the first ten eigenvectors.

3.6. Cosine Content Calculation

The cosine content was calculated for both the apo and the holo LasR protein simulations to evaluate the degree of randomness shown by the first 10 eigenvectors. Both the apo and holo LasR proteins were found to have a cosine content of less than 0.2 (Figure 13). The Root Mean Square Inner Product (RMSIP) reveals a low degree of overlap (22.1 %) between the two subspaces (the first three eigenvectors). The RMSIP also indicated that there was a similarity of 40.9 % between the C matrices of apo and holo LasR proteins, indicating that the sampling was comparable across the two systems.

Figure 13. Values of the cosine content of the first ten eigenvectors for the two trajectories.

3.7. Bi-Dimensional Projection Calculations

The projections of these trajectories onto the first three eigenvectors of the updated C matrix are shown in Figure 14. In each of these diagrams, the bigger dot depicts the average structure of the relevant trajectory. Figure 14A, a projection on the first two eigenvectors, reveals that the two trajectories have distinct average structures and that the frames overlap at the simulation's last frames (dark red and black dots). Figure 14B shows that the two paths intersect

(at the end of the simulation) and that their average structures are more comparable than in the prior projection. Finally, Figure 14C (projection on the second and third eigenvectors) shows that there are a lot of variances between the sampled frames and a similar projection with overlap at the simulation's last frame. Porcupine diagrams were used to illustrate the motion of the first three eigenvectors (Figure 15). The red holo LasR protein structure shows that the binding pocket is slightly closing in the first three PCs, whereas the green apo LasR protein structure indicates a little opening.

Figure 14. The projection of each trajectory on **A)** the first two eigenvectors, **B)** the first and third eigenvectors, and **C)** the second and third eigenvectors.

Figure 15. The porcupine figures of each of the first three eigenvectors for both systems. red cartoon: holo LasR protein trajectory, green cartoon: apo LasR protein trajectory.

***In vitro* Studies**

3.8. Patuletin MIC determination

By using the broth micro-dilution technique, the MIC of Patuletin was found to be 4 mg/ml. The further possible anti-virulence effects of Patuletin against *P. aeruginosa* virulence factors activities were examined at a sub-MIC concentration equivalent to ¼ MIC (1 mg/ml) as other sub-inhibitory concentrations did not show any inhibitory impact and to exclude any potential inhibitory activity of the tested substance due to the possible lethal activity on bacterial growth.

Impact of sub-MIC of Patuletin on virulence factors in *P. aeruginosa*

3.10. Biofilm inhibition assessment

In this study, the crystal violet technique was used to assess the inhibitory effect of Patuletin on biofilm formation. Interestingly, Patuletin significantly reduced biofilm formation ability from 100% in untreated isolates to 48% and 42% in PA27853-treated isolate and PA1-treated isolate, respectively (**Figure 16**).

Figure16. Patuletin at 1/4 MIC significantly decreased *P. aeruginosa* ability to produce biofilms in treated bacteria as compared to control untreated bacteria. Optical density was measured at 570 nm. The data shown represent the means ± standard errors. *P < 0.05.

3.11. Pyocyanin inhibition assessment

The ability of Patuletin to inhibit pyocyanin pigment production in *P. aeruginosa* was estimated spectrophotometrically. Importantly, Patuletin significantly decreased pyocyanin production from 100% in untreated isolates to 76% and 86% in PA27853-treated isolate and PA1-treated isolate, respectively (**Figure 17**).

Figure 17. Patuletin at 1/4 MIC significantly reduced the production of pyocyanin in *P. aeruginosa* in treated isolates compared to control untreated isolates. Optical density was measured at 570 nm. The data shown represent the means of three biological experiments ± standard errors. *P < 0.05.

3.12. Proteases inhibition assessment

The modified skim milk assay technique was used to test the proteolytic activity both with and without sub-MIC concentration of Patuletin. Significantly Patuletin decreased the proteolytic activity from 100% in untreated isolates to 58% and 80% in PA27853-treated isolate and PA1-treated isolate, respectively (**Figure 18**).

Figure 18. In Patuletin-treated isolates, a significant decrease in proteases activity was observed. OD_{600} was measured following overnight culturing of bacteria in LB broth with and without 1/4 MIC of Patuletin followed by incubation of supernatants with skim milk for ½ hr at 37 °C. The data shown are the means ± standard errors of three biological experiments with three technical replicates each. *, significant P < 0.05

The obtained results suggest that Patuletin has significant effects on biofilm formation, pyocyanin production, and proteolytic activity in PA27853 and PA1 bacterial strains. Interstingly, these resuls were consistent with several published results on other flavonoids. For instance, a study by Ouyang et al. investigated the effects of quercetin, a widely studied flavonoid, on biofilm formation in *P. aeruginosa*. They reported a significant reduction in biofilm formation with the ratios of 36, 51, 28 and 20% at the concentration of 8, 16, 32 and 64 µg /ml, respectively [33]. In another study, At a concentration of 0.5 MIC quercetin potently reduced *P. aeruginosa* biofilm formation and twitching motility by a ratio of 95% [60]. Similarly, luteolin cotrolled the biofilm

formation of *P. aeruginosa* at 62.5, 125, and 250 µg/mL[61]. These findings suggest that multiple flavonoids, including Patuletin and quercetin, have the potential to disrupt biofilm formation, which is a crucial step in bacterial colonization and virulence.

Regarding pyocyanin production, Olivier et al. reported the significant reductions in pyocyanin production by Naringenin, Eriodictyol and Taxifolin (2 mM) on PAO1 strain by ratios of 86.8±1.4%, 73.2±5.2% and 55.8±8.1%, respectively [62]. Also, calycopterin inhibited pyocyanin production at a concentration of 32 µM [63]. It is evident that different flavonoids may exhibit varying degrees of inhibition suggesting that the specific structure of flavonoids could influence its effectiveness against *P. aeruginosa*. In a recent study, Hispidulin at a concentration of 75 µg/ml decreased pyocyanin pigment production of reporter bacteria and test bacteria to 81.92 and 71.69 %, respectively [32]. Marked decrease in biofilm formation, pyocyanin production and proteolytic activity of *P.s aeruginosa* was reported in presence of 110 µg/ml of the flavonoide vitexin in combination with azithromycin [64].

4. Conclusion

In conclusion, the findings of this study highlight the promising potential of Patuletin as a LasR and vieulence factors inhibitor in the context of combating *P. aeruginosa* infections. Through a comprehensive analysis utilizing computational and experimental approaches, Patuletin demonstrated a strong binding affinity to LasR, ensuring the stability of the Patuletin -LasR complex. Moreover, Patuletin exhibited significant *In vitro* inhibitory effects on crucial aspects of *P. aeruginosa* virulence, including biofilm formation, pyocyanin production, and protease activity. These findings hold considerable promise for the development of innovative strategies to combat antibiotic-tolerant *P. aeruginosa* infections. Patuletin 's ability to inhibit LasR activity and attenuate crucial virulence factors suggest its potential as a targeted therapeutic alternaive or adjuvnt agent to traditional antibiotics. The results encourage further exploration of Patuletin as a promising for candidate the development of novel antibacterial agents against drug-resistant *P. aeruginosa* strains.

Funding: This research was funded by Princess Nourah bint Abdulrahman University Researchers Supporting Project number (PNURSP2023R116), Princess Nourah bint Abdulrahman University, Riyadh, Saudi Arabia. The authors extend their appreciation to the Research Center at AlMaarefa University for funding this work.

Institutional Review Board Statement: Not applicable

Ethical Approval Statement: There is no ethical issue regarding this work.

Informed Consent Statement: Not applicable

Data Availability Statement: Data are available with corresponding authors upon request

Conflicts of Interest: No conflict of interest is to be stated

Sample Availability: Patuletin is available from the authors.

Authors' contributions: The study was conceptualized and designed by AMM, IHE, and MMS. MMS did the microbiological studies. MA, AAA, and EBK participated in the experiments. HE and IMI conducted the computational studies. The funding was obtained by EBE and AAA, who also contributed to writing the manuscript with MA. All authors have thoroughly reviewed and approved the final manuscript, taking responsibility for its scientific validity, and originality, and ensuring it meets the required standards for similarity index.

References

1. Wu, W., et al., *Pseudomonas aeruginosa*, in *Molecular medical microbiology*. 2015, Elsevier. p. 753-767.
2. Silby, M.W., et al., *Pseudomonas genomes: diverse and adaptable.* 2011. **35**(4): p. 652-680.
3. Lau, G.W., et al., *The role of pyocyanin in Pseudomonas aeruginosa infection.* 2004. **10**(12): p. 599-606.
4. Hoge, R., et al., *Weapons of a pathogen: proteases and their role in virulence of Pseudomonas aeruginosa.* 2010. **2**: p. 383-395.
5. Galdino, A.C.M., et al., *Pseudomonas aeruginosa and its arsenal of proteases: weapons to battle the host.* 2017: p. 381-397.
6. Thi, M.T.T., D. Wibowo, and B.H.J.I.j.o.m.s. Rehm, *Pseudomonas aeruginosa biofilms.* 2020. **21**(22): p. 8671.
7. Aloush, V., et al., *Multidrug-resistant Pseudomonas aeruginosa: risk factors and clinical impact.* 2006. **50**(1): p. 43-48.
8. Sun, E. and F.E.J.G. Cohen, *Computer-assisted drug discovery—a review.* 1993. **137**(1): p. 127-132.
9. Padole, S.S., et al., *A review of approaches in computer-aided drug design in drug discovery.* 2022. **19**(2): p. 075-083.
10. Eissa, I.H., et al., *Ligand and structure-based in silico determination of the most promising SARS-CoV-2 nsp16-nsp10 2'-o-Methyltransferase complex inhibitors among 3009 FDA approved drugs.* Molecules, 2022. **27**(7): p. 2287.
11. Mohammed, S.O., et al., *Expression, Purification, and Comparative Inhibition of Helicobacter pylori Urease by Regio-Selectively Alkylated Benzimidazole 2-Thione Derivatives.* Molecules, 2022. **27**(3): p. 865.
12. Suleimen, Y.M., et al., *Jusanin, a New Flavonoid from Artemisia commutata with an In Silico Inhibitory Potential against the SARS-CoV-2 Main Protease.* Molecules, 2022. **27**(5): p. 1636.
13. Suleimen, Y.M., et al., *Isolation and In Silico SARS-CoV-2 Main Protease Inhibition Potential of Jusan Coumarin, a New Dicoumarin from Artemisia glauca.* Molecules, 2022. **27**(7): p. 2281.

14. Eissa, I.H., et al., *In silico exploration of potential natural inhibitors against SARS-Cov-2 nsp10.* Molecules, 2021. **26**(20): p. 6151.
15. Elkaeed, E.B., et al., *Multi-Phase In Silico Discovery of Potential SARS-CoV-2 RNA-Dependent RNA Polymerase Inhibitors among 3009 Clinical and FDA-Approved Related Drugs.* Processes, 2022. **10**(3): p. 530.
16. Suleimen, Y.M., et al., *Isolation and In Silico Anti-SARS-CoV-2 Papain-Like Protease Potentialities of Two Rare 2-Phenoxychromone Derivatives from Artemisia spp.* Molecules, 2022. **27**(4): p. 1216.
17. Alesawy, M.S., et al., *In Silico Screening of Semi-Synthesized Compounds as Potential Inhibitors for SARS-CoV-2 Papain-like Protease: Pharmacophoric Features, Molecular Docking, ADMET, Toxicity and DFT Studies.* Molecules, 2021. **26**(21): p. 6593.
18. Liu, H.B., et al., *Characterization of LasR protein involved in bacterial quorum sensing mechanism of Pseudomonas aeruginosa.* 2009. **14**: p. 146-154.
19. Rex, D.A.B., et al., *Pleotropic potential of quorum sensing mediated N-acyl homoserine lactones (AHLs) at the LasR and RhlR receptors of Pseudomonas aeruginosa.* 2022: p. 1-13.
20. Kiratisin, P., K.D. Tucker, and L.J.J.o.b. Passador, *LasR, a transcriptional activator of Pseudomonas aeruginosa virulence genes, functions as a multimer.* 2002. **184**(17): p. 4912-4919.
21. Chowdhury, N. and A.J.G. Bagchi, *Molecular insight into the activity of LasR protein from Pseudomonas aeruginosa in the regulation of virulence gene expression by this organism.* 2016. **580**(1): p. 80-87.
22. Metwaly, A.M., et al., *Traditional ancient Egyptian medicine: a review.* Saudi Journal of Biological Sciences, 2021.
23. Han, X., et al., *The Chinese herbal formulae (Yitangkang) exerts an antidiabetic effect through the regulation of substance metabolism and energy metabolism in type 2 diabetic rats.* Journal of ethnopharmacology, 2019. **239**: p. 111942.
24. Newman, D.J. and G.M.J.J.o.n.p. Cragg, *Natural products as sources of new drugs from 1981 to 2014.* 2016. **79**(3): p. 629-661.
25. Metwaly, A.M., et al., *Black ginseng and its saponins: Preparation, phytochemistry and pharmacological effects.* 2019. **24**(10): p. 1856.
26. Rao, P.S. and T. Seshadri. *The colouring matter of the flowers ofTagetes patula: Isolation of a new flavonol, patuletin and its constitution*. in *Proceedings of the Indian Academy of Sciences-Section A*. 1941. Springer.
27. Abdel-Wahhab, M.A., A. Said, and A. Huefner, *NMR and radical scavenging activities of patuletin from Urtica urens. Against aflatoxin B1.* Pharm Biol, 2005. **43**(6): p. 515-525.
28. Bate-Smith, E. and J. Harborne, *Quercetagetin and patuletin in Eriocaulon.* Phytochemistry, 1969. **8**(6): p. 1035-1037.
29. Faizi, S., et al., *Antibacterial and antifungal activities of different parts of Tagetes patula.: Preparation of patuletin derivatives.* 2008. **46**(5): p. 309-320.
30. Tereschuk, M.a.L., et al., *Antimicrobial activity of flavonoids from leaves of Tagetes minuta.* 1997. **56**(3): p. 227-232.
31. Górniak, I., R. Bartoszewski, and J.J.P.r. Króliczewski, *Comprehensive review of antimicrobial activities of plant flavonoids.* 2019. **18**: p. 241-272.
32. Anju, V., et al., *In vivo, in vitro and molecular docking studies reveal the anti-virulence property of hispidulin against Pseudomonas aeruginosa through the modulation of quorum sensing.* 2022. **174**: p. 105487.
33. Ouyang, J., et al., *Quercetin is an effective inhibitor of quorum sensing, biofilm formation and virulence factors in Pseudomonas aeruginosa.* 2016. **120**(4): p. 966-974.
34. Grabski, H. and S. Tiratsuyan. *Interaction of quercetin with LasR of Pseudomonas aeruginosa: mechanistic insights of the inhibition of virulence through quorum sensing*. in *4th International*

Conference on Nanotechnologies and Biomedical Engineering: Proceedings of ICNBME-2019, September 18-21, 2019, Chisinau, Moldova. 2020. Springer.

35. Geng, Y.F., et al., *An innovative role for luteolin as a natural quorum sensing inhibitor in Pseudomonas aeruginosa.* Life Sciences, 2021. **274**: p. 119325.
36. Hernando-Amado, S., et al., *Naringenin inhibition of the Pseudomonas aeruginosa quorum sensing response is based on its time-dependent competition with N-(3-Oxo-dodecanoyl)-L-homoserine lactone for LasR binding.* 2020. **7**: p. 25.
37. Grabski, H. and S.J.b. Tiratsuyan, *Mechanistic insights of the attenuation of quorum-sensing-dependent virulence factors of Pseudomonas aeruginosa: Molecular modeling of the interaction of taxifolin with transcriptional regulator LasR.* 2018: p. 500157.
38. Chaieb, K., et al., *Computational screening of natural compounds as putative quorum sensing inhibitors targeting drug resistance bacteria: Molecular docking and molecular dynamics simulations.* Computers in Biology and Medicine, 2022. **145**: p. 105517.
39. Smith, R.S. and B.H.J.T.J.o.c.i. Iglewski, *Pseudomonas aeruginosa quorum sensing as a potential antimicrobial target.* 2003. **112**(10): p. 1460-1465.
40. Suleimen, Y.M., et al., *Isolation and In Silico Inhibitory Potential against SARS-CoV-2 RNA Polymerase of the Rare Kaempferol 3-O-(6 ”-O-acetyl)-Glucoside from Calligonum tetrapterum.* 2022. **11**(15): p. 2072.
41. Abraham, M.J., et al., *GROMACS: High performance molecular simulations through multi-level parallelism from laptops to supercomputers.* 2015. **1**: p. 19-25.
42. Brooks, B.R., et al., *CHARMM: the biomolecular simulation program.* 2009. **30**(10): p. 1545-1614.
43. Jo, S., et al., *CHARMM-GUI PDB manipulator for advanced modeling and simulations of proteins containing nonstandard residues.* 2014. **96**: p. 235-265.
44. Tuccinardi, T.J.E.o.o.d.d., *What is the current value of MM/PBSA and MM/GBSA methods in drug discovery?* 2021. **16**(11): p. 1233-1237.
45. Valdés-Tresanco, M.S., et al., *gmx_MMPBSA: a new tool to perform end-state free energy calculations with GROMACS.* 2021. **17**(10): p. 6281-6291.
46. Amadei, A., et al., *Essential dynamics of proteins.* 1993. **17**(4): p. 412-425.
47. Papaleo, E., et al., *Free-energy landscape, principal component analysis, and structural clustering to identify representative conformations from molecular dynamics simulations: the myoglobin case.* 2009. **27**(8): p. 889-899.
48. Metwaly, A.M., et al., *The computational preventive potential of the rare Flavonoid, Patuletin, isolated from Tagetes patula, against SARS-CoV-2.* 2022. **11**(14): p. 1886.
49. Patel, J.B., *Performance standards for antimicrobial susceptibility testing; twenty-fifth informational supplement*. 2015, Clinical and Laboratory Standards Institute.
50. Stepanović, S., et al., *Quantification of biofilm in microtiter plates: overview of testing conditions and practical recommendations for assessment of biofilm production by staphylococci.* Apmis, 2007. **115**(8): p. 891-9.
51. Das, T. and M. Manefield, *Pyocyanin promotes extracellular DNA release in Pseudomonas aeruginosa.* 2012.
52. El-Mowafy, S.A., et al., *Aspirin is an efficient inhibitor of quorum sensing, virulence and toxins in Pseudomonas aeruginosa.* 2014. **74**: p. 25-32.
53. Liu, X., et al., *Molecular dynamics simulations and novel drug discovery.* 2018. **13**(1): p. 23-37.
54. Hollingsworth, S.A. and R.O.J.N. Dror, *Molecular dynamics simulation for all.* 2018. **99**(6): p. 1129-1143.
55. Zhao, Z. and P.E.J.D.D.T. Bourne, *Harnessing systematic protein–ligand interaction fingerprints for drug discovery.* 2022.

~~56. Xiong, G., et al., *Featurization strategies for protein–ligand interactions and their applications in scoring function development.* 2022. **12**(2): p. e1567.~~

~~57. Salentin, S., et al., *From malaria to cancer: Computational drug repositioning of amodiaquine using PLIP interaction patterns.* 2017. **7**(1): p. 11401.~~

~~58. Salentin, S., et al., *PLIP: fully automated protein–ligand interaction profiler.* 2015. **43**(W1): p. W443-W447.~~

~~59. Tubiana, T., et al., *TTClust: a versatile molecular simulation trajectory clustering program with graphical summaries.* 2018. **58**(11): p. 2178-2182.~~

60. Pejin, B., et al., *Quercetin potently reduces biofilm formation of the strain Pseudomonas aeruginosa PAO1 in vitro.* 2015. **16**(8): p. 733-737.

61. Rivera, M.L.C., et al., *Effect of Capsicum frutescens extract, capsaicin, and luteolin on quorum sensing regulated phenotypes.* 2019. **84**(6): p. 1477-1486.

62. Vandeputte, O.M., et al., *The flavanone naringenin reduces the production of quorum sensing-controlled virulence factors in Pseudomonas aeruginosa PAO1.* 2011. **157**(7): p. 2120-2132.

63. Froes, T.Q., et al., *Calycopterin, a major flavonoid from Marcetia latifolia, modulates virulence-related traits in Pseudomonas aeruginosa.* 2020. **144**: p. 104142.

64. Das, M.C., et al., *Attenuation of Pseudomonas aeruginosa biofilm formation by Vitexin: a combinatorial study with azithromycin and gentamicin.* 2016. **6**(1): p. 23347.

Figure 1

Chemical structures of Patuletin, cocrystallized ligand (TY4) and reported flavonoid inhibitors of LasR protein

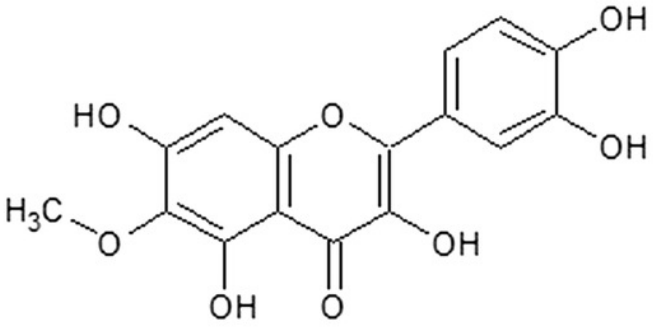

Pt

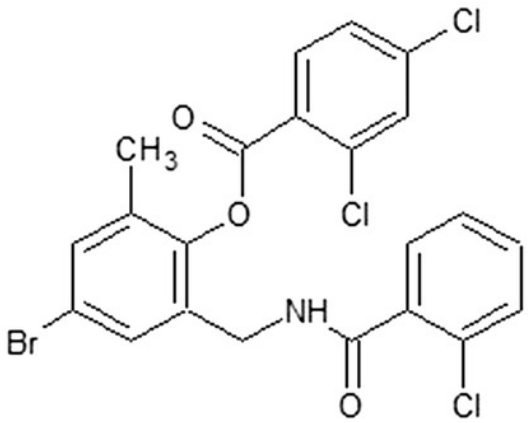

TY4

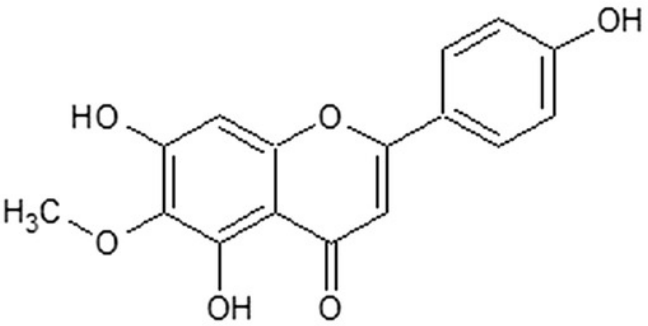

Hispidulin

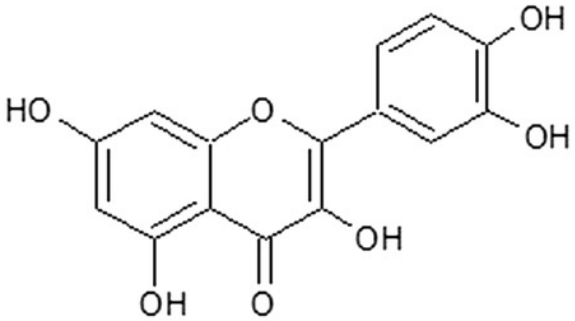

Quercetin

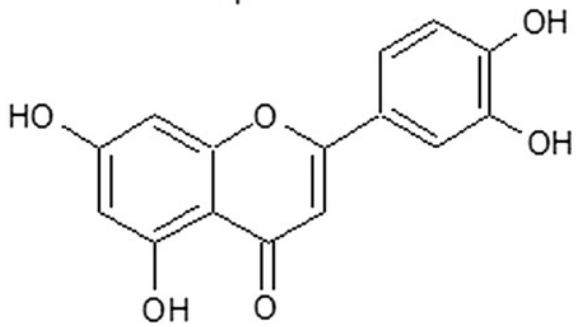

Luteolin

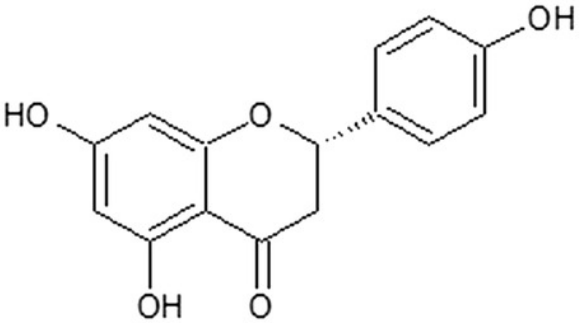

Naringenin

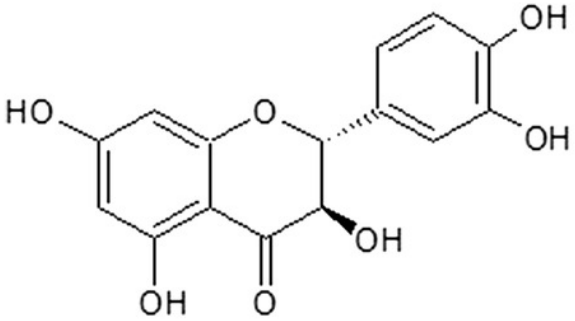

Taxifolin

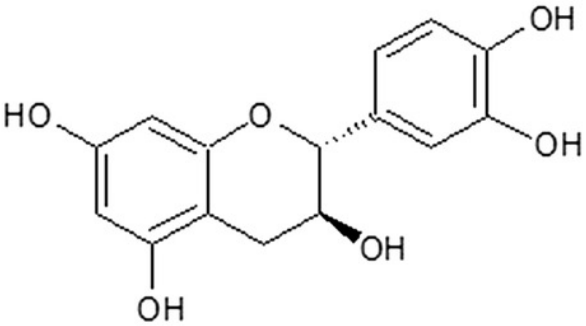

Catechin

Figure 2

Superimposition of the docked pose (blue) and the co-crystallized one (pink) inside of the active site of LasR protein with an RMSD value 0.40 Å

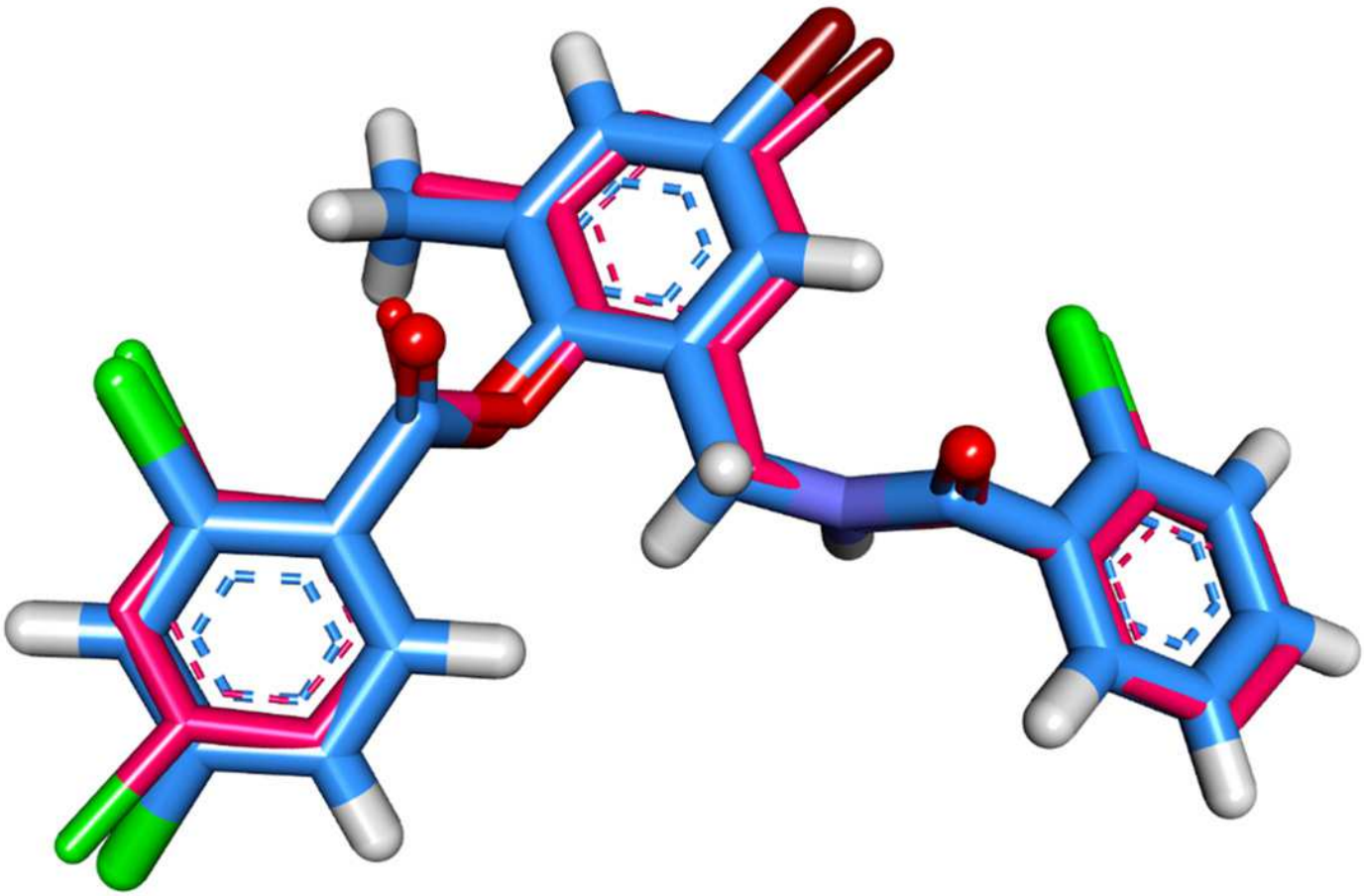

Figure 3

A) 3D interaction of the co-crystallized ligand (TY4) in the active site of the LasR protein. B) 2D interaction of TY4 in the active site of LasR protein. C) Mapping surface showing TY4 occupying the active site of LasR protein

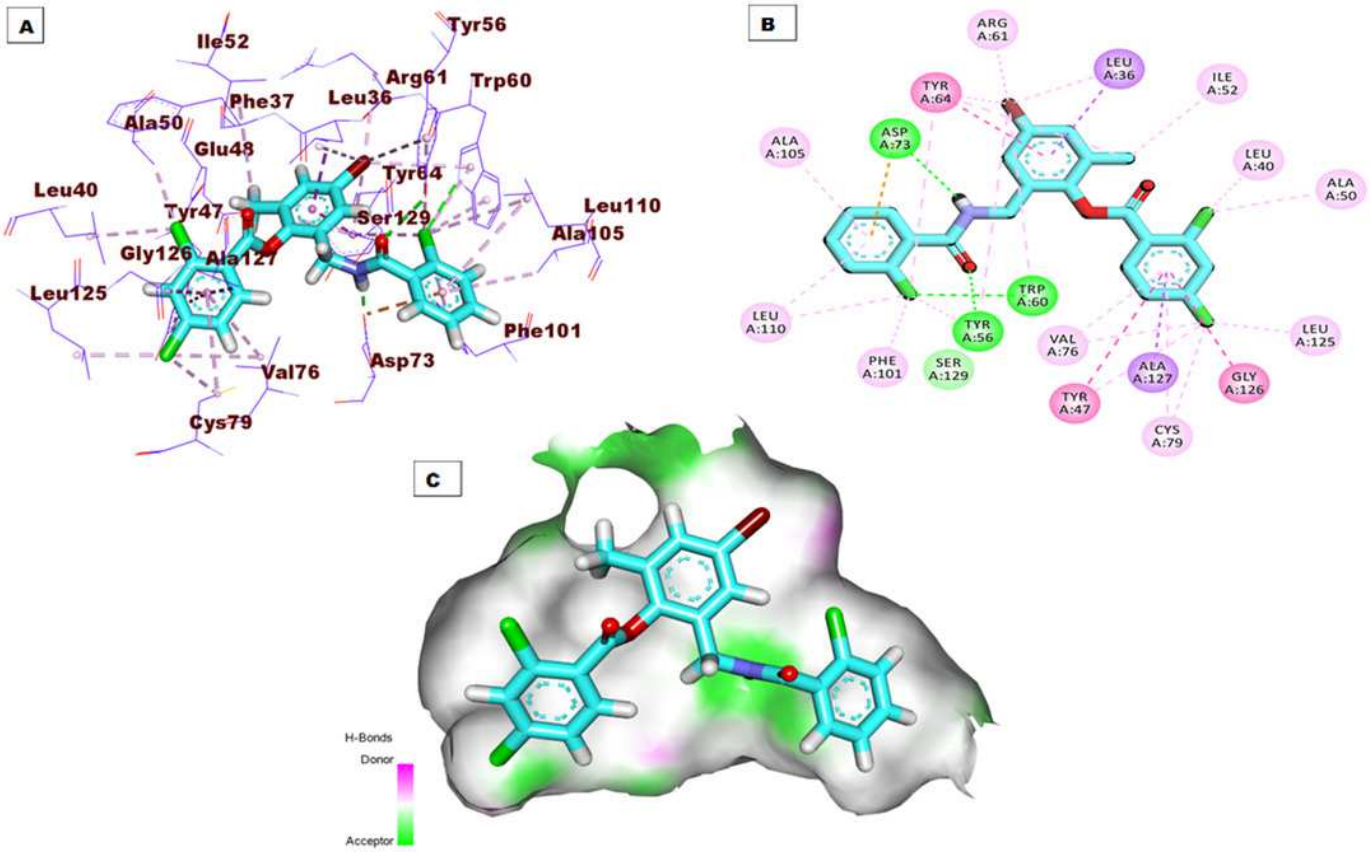

Figure 4

A) 3D interaction of Patuletin in the active site of LasR protein. B) 2D interaction of Patuletin in the active site of LasR protein. C) Mapping surface showing Patuletin occupying the active site of LasR protein.

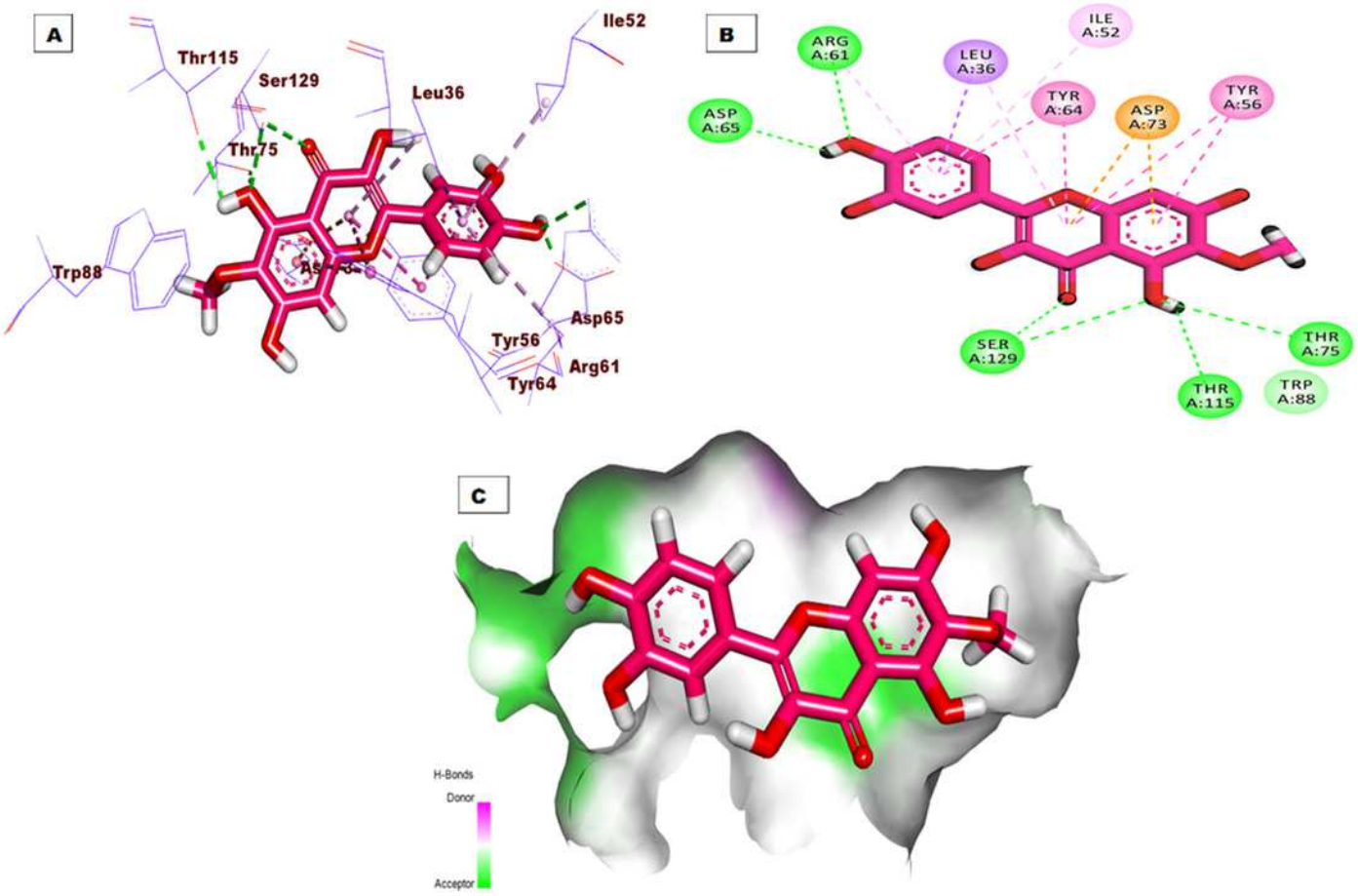

Figure 5

A) RMSD values from the trajectory for the LasR protein, B) shows Plateulin RMSD values, C) radius of gyration, D) SASA, E) change in the number of hydrogen bonds, F) RMSF, G) distance from the center of mass of Plateulin compound and LasR protein.

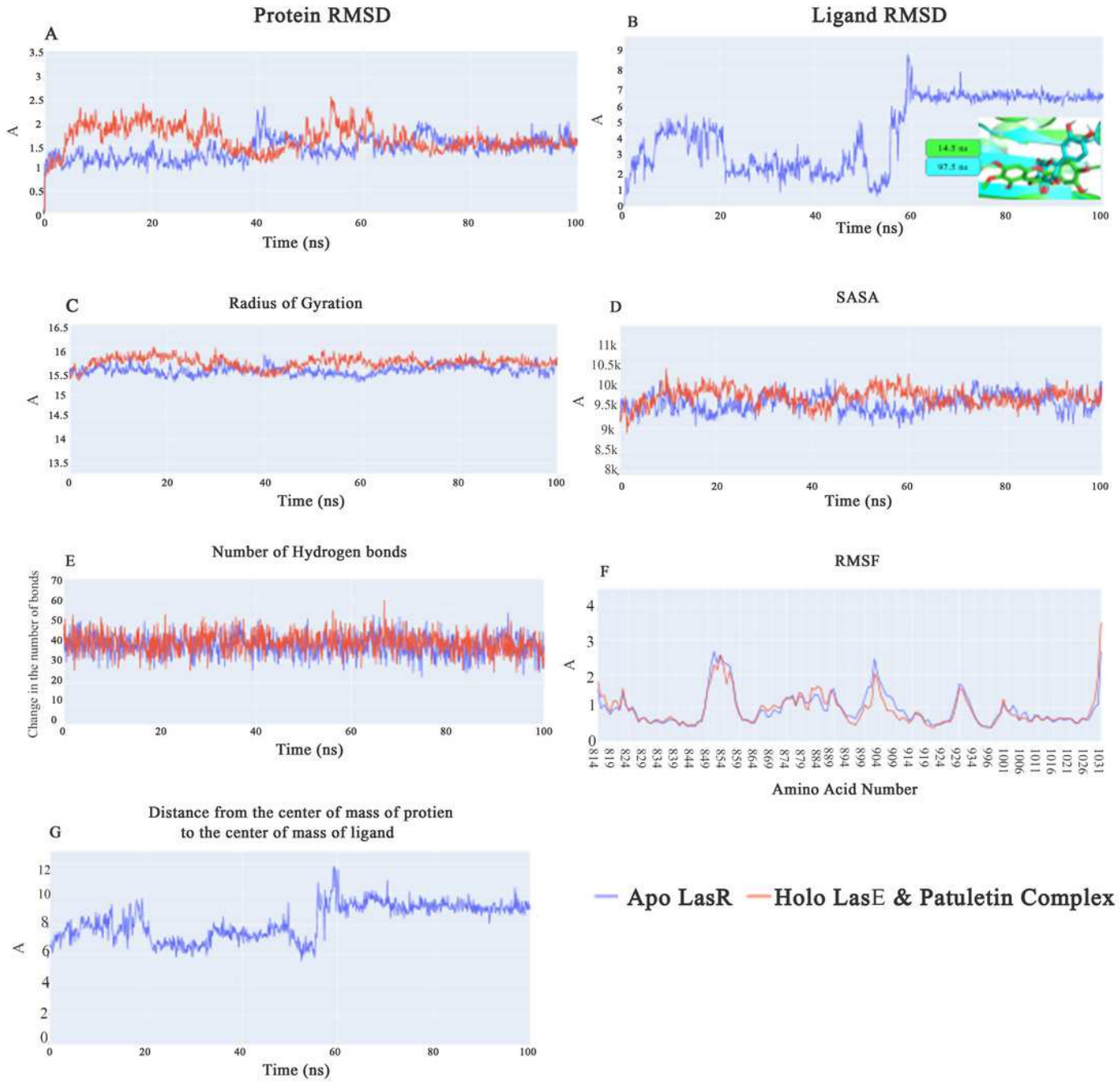

Figure 6

Energetic components of MM-GBSA and their values. Bars represent the standard deviations

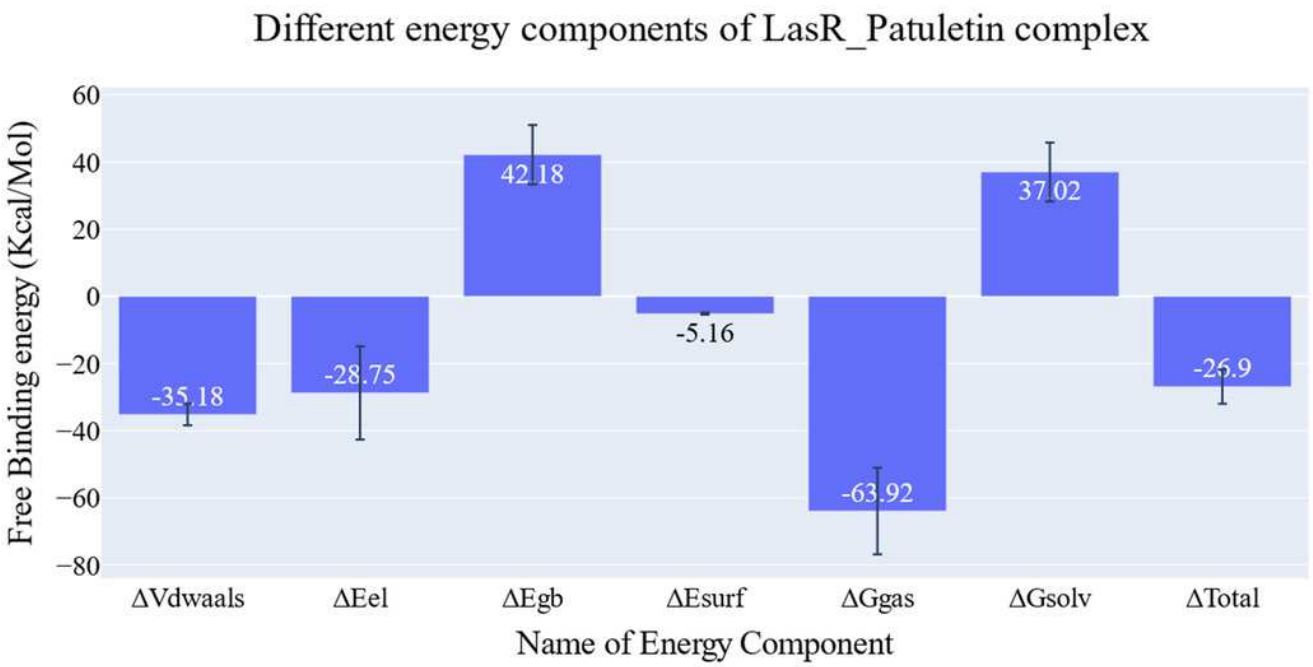

Figure 7

Binding free energy decomposition of the Plateulin -LasR complex

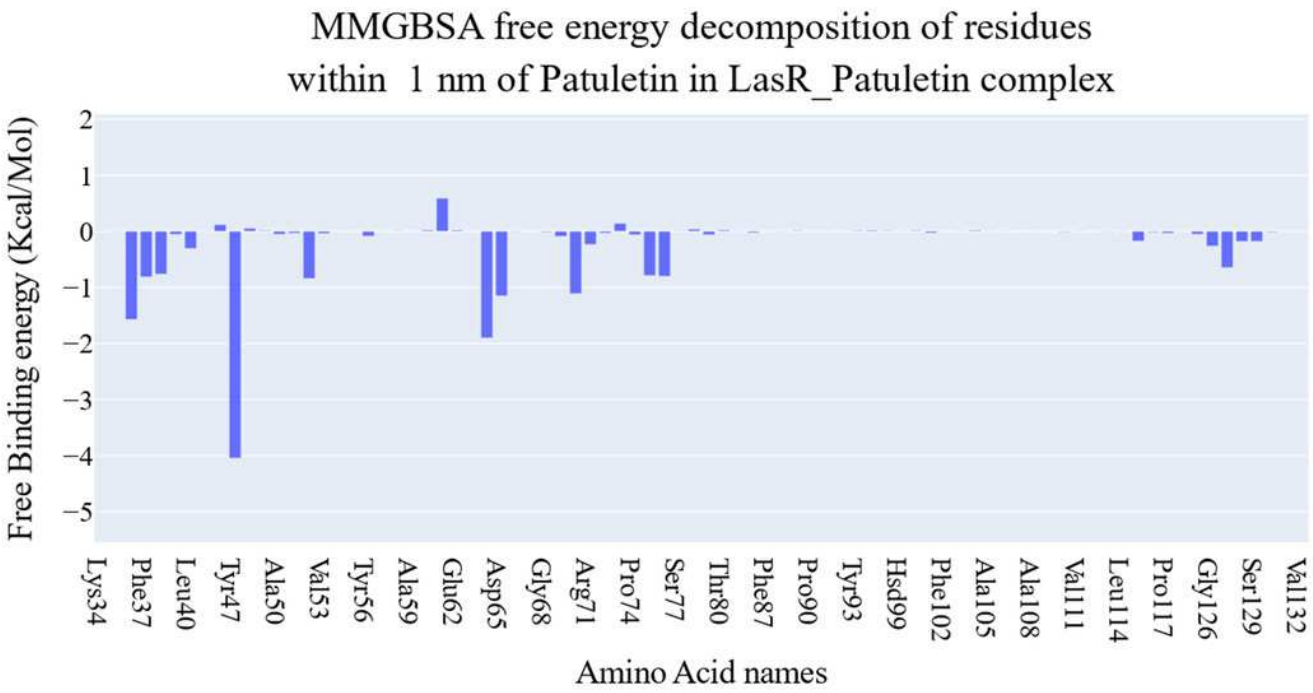

Figure 8

The amino acids, the types of interactions with Plateulin, and their occurrence during the whole simulation time using the ProLIF Python library

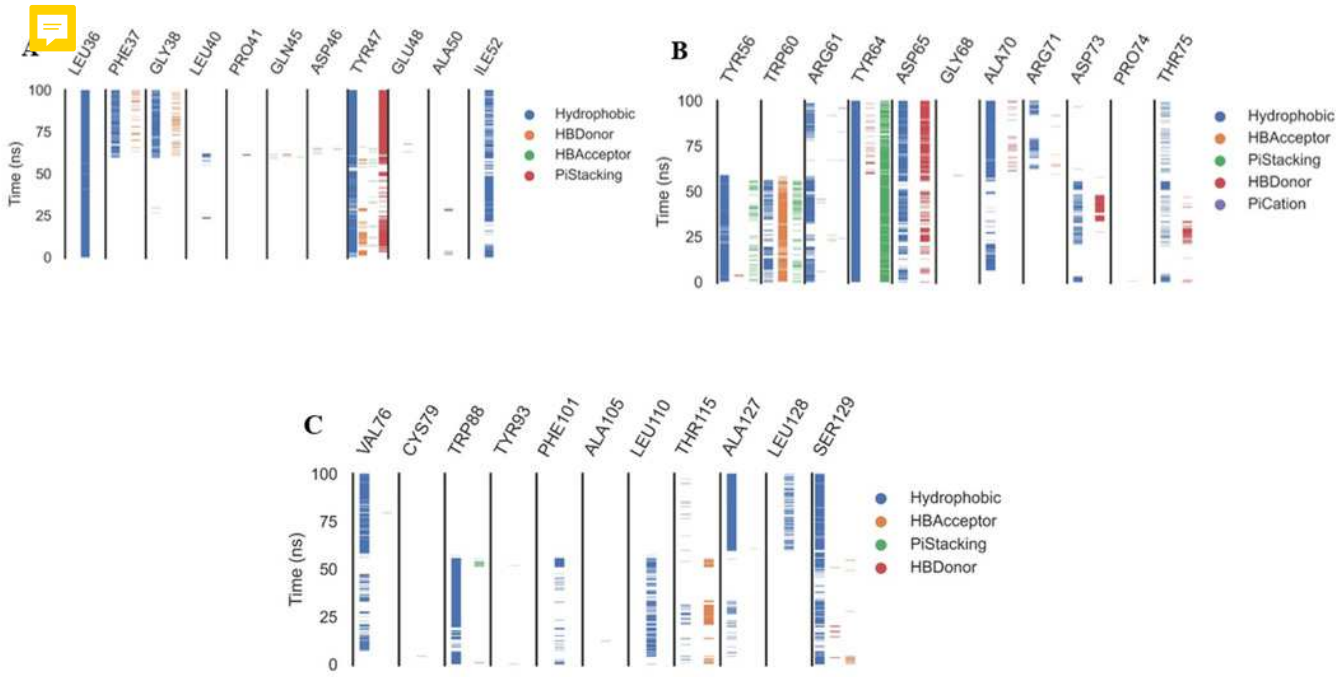

Figure 9

The four clusters representative obtained from TTClust and their 3D interactions with Plateulin.

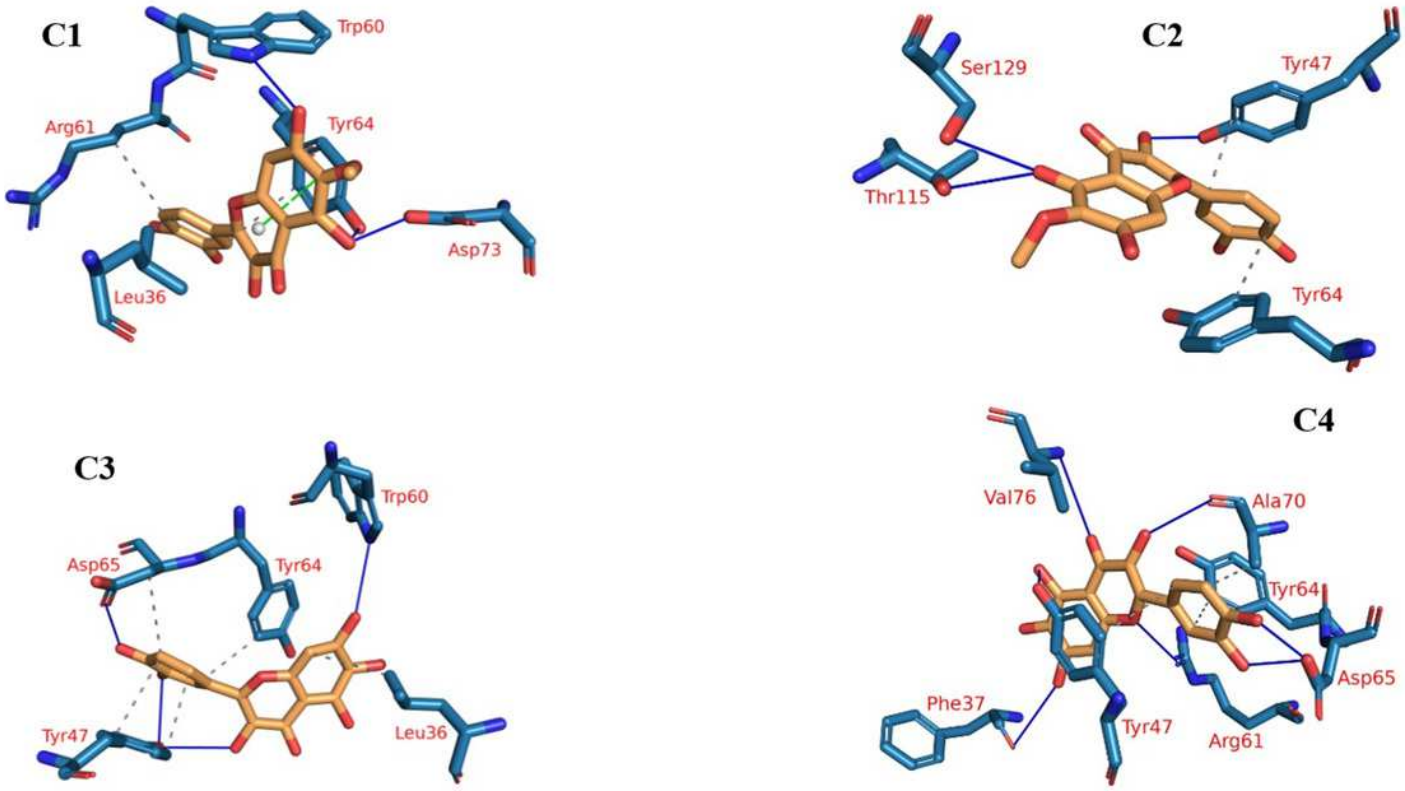

Figure 10

A) The change in the distances of three key interactions (as obtained from ProLIF and PLIP). Blue line: shows the distance between Leu36 and atom C13 in Plateulin, Red Line: shows the distance between Leu36 and atom C6 in Plateulin, and Green line: shows

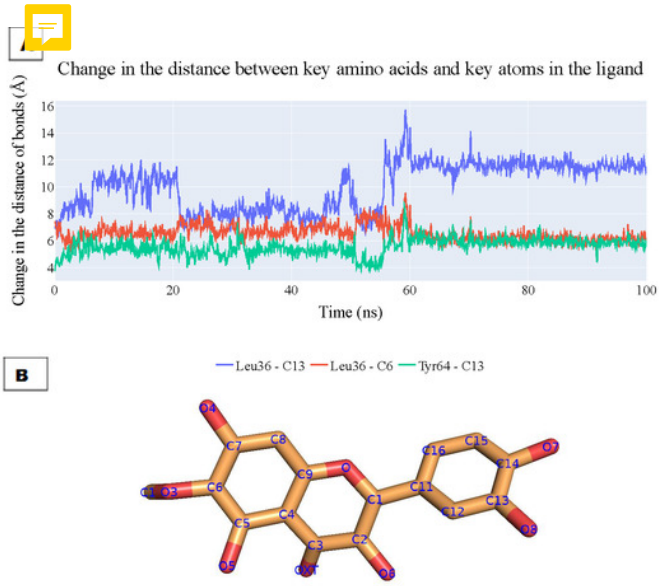

Figure 11

The change in the eigenvalues with increasing the eigenvectors (blue line). In addition, the cumulative variance retained in the eigenvectors is shown (red line)

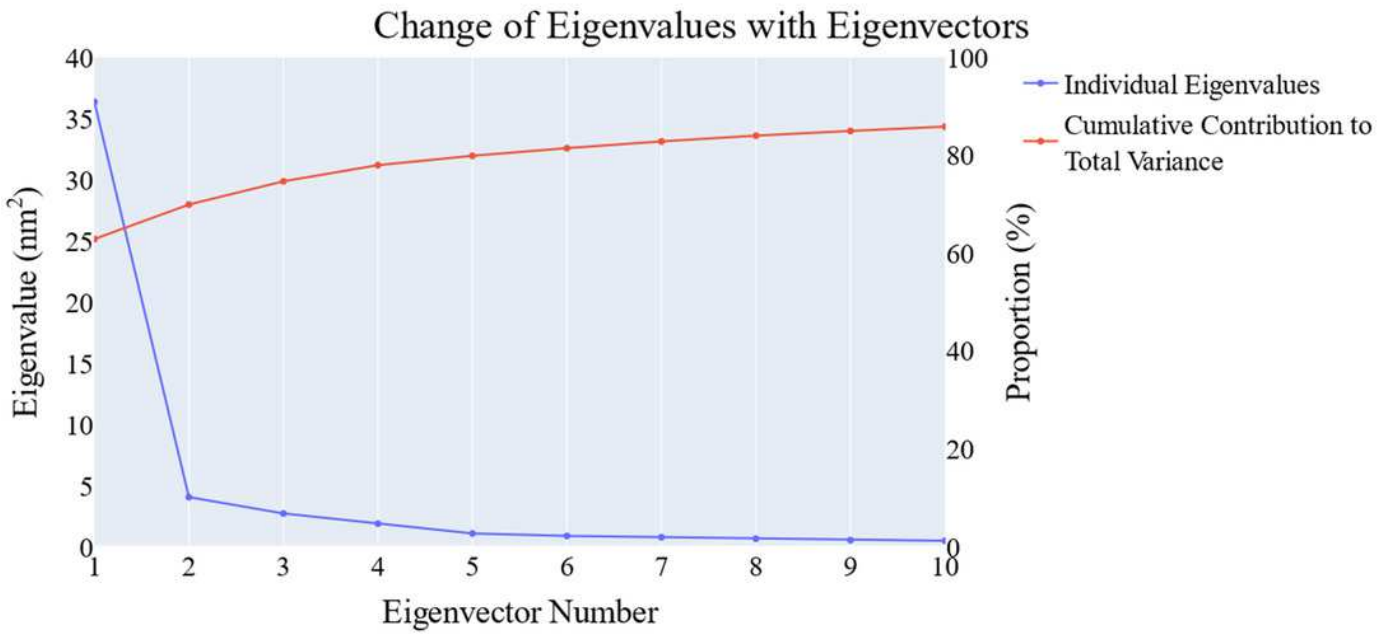

Figure 12

The distribution of the 1st ten eigenvectors

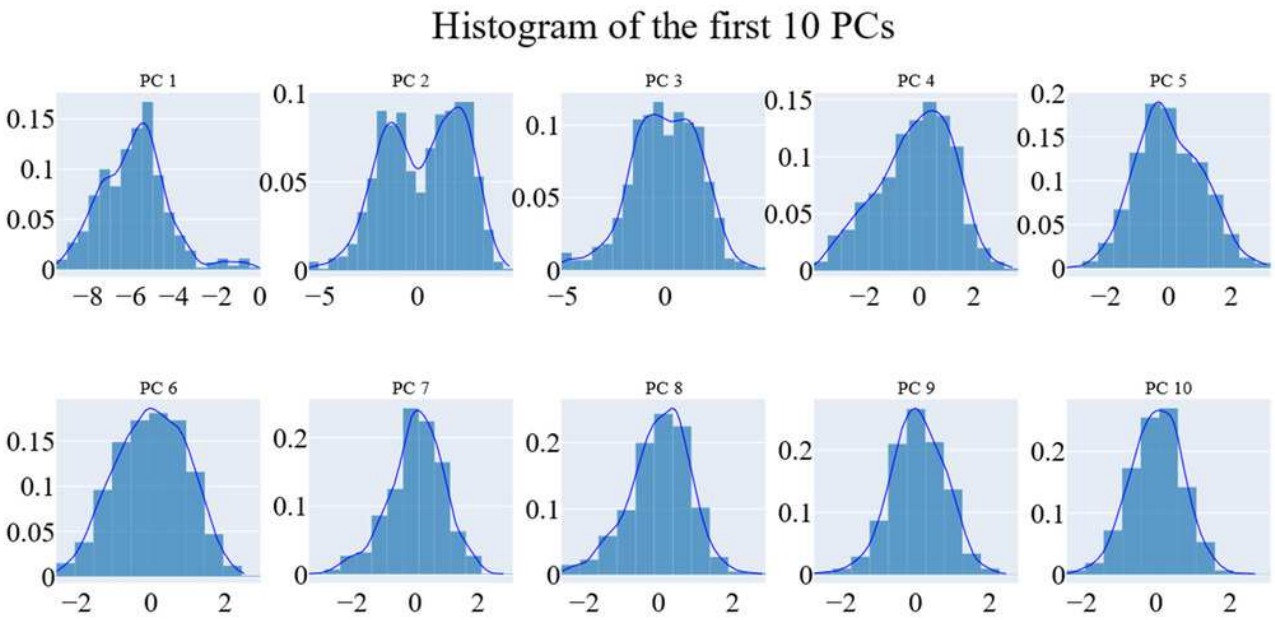

Figure 13

Values of the cosine content of the 1st ten eigenvectors for the two trajectories

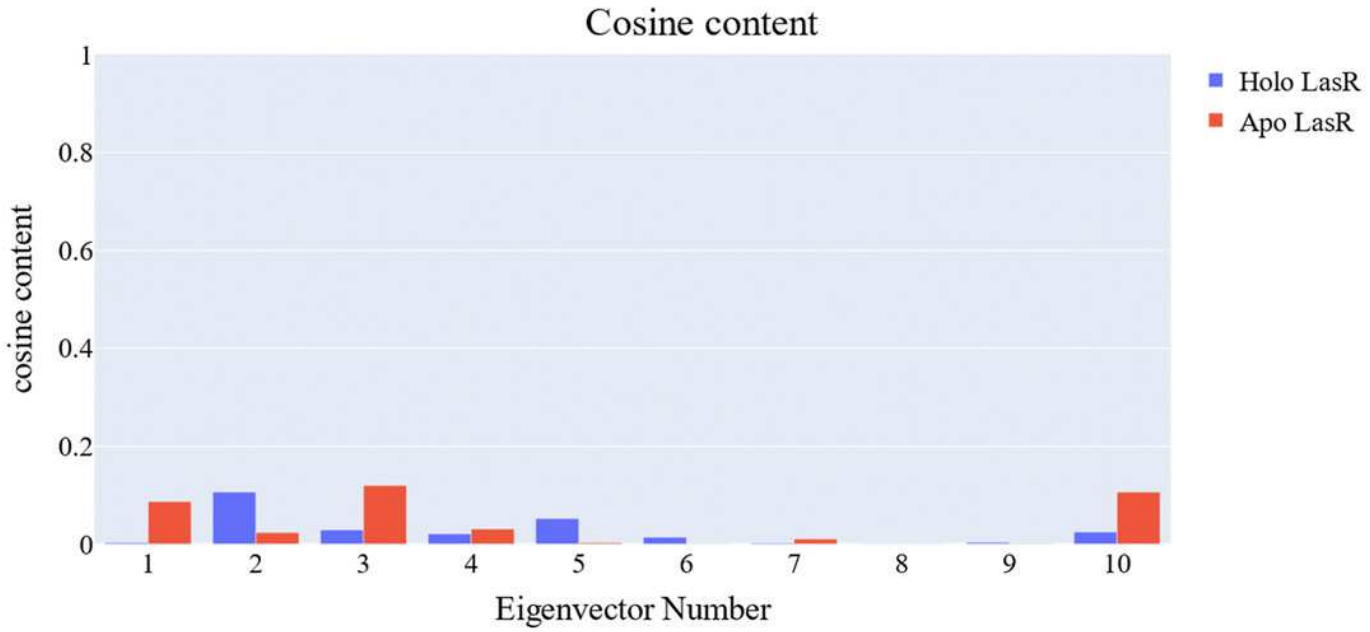

Figure 14

The projection of each trajectory on A) the first two eigenvectors, B) the first and third eigenvectors, and C) the second and third eigenvectors

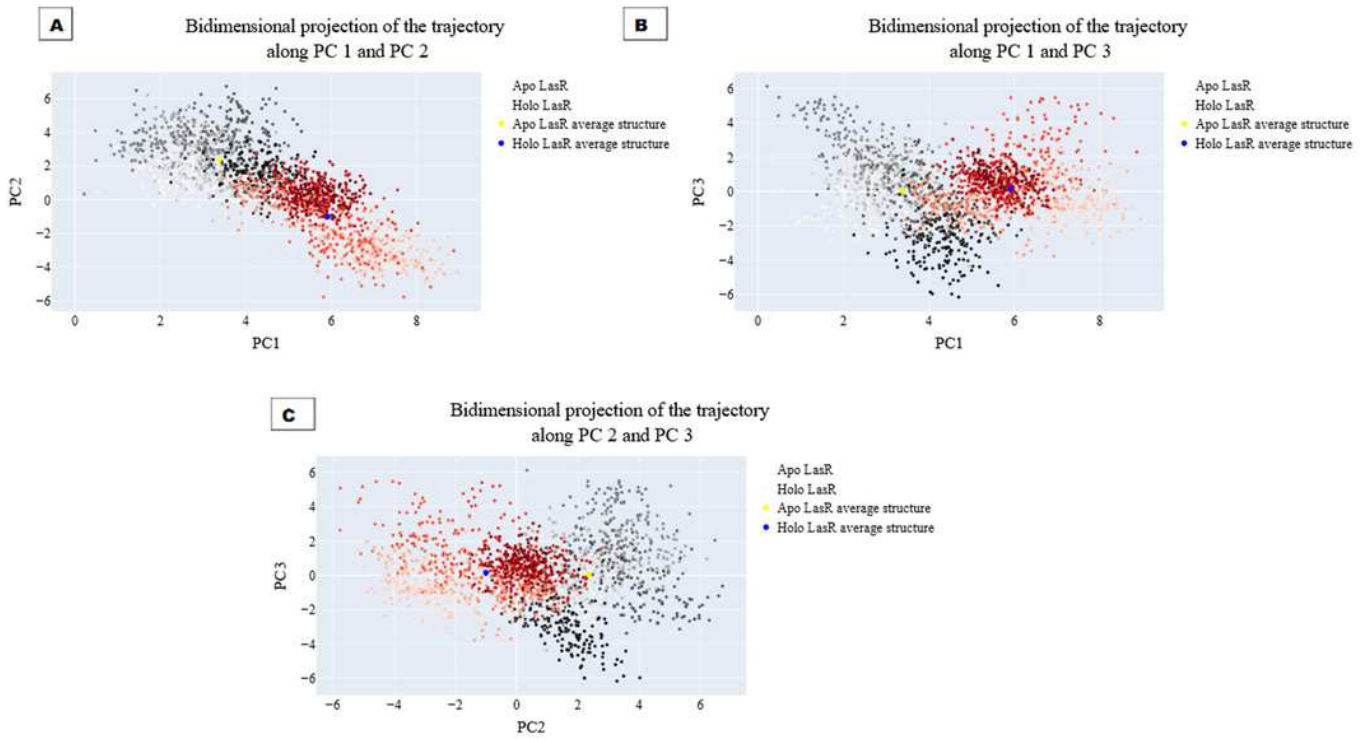

Figure 15

The porcupine figures of each of the first three eigenvectors for both systems. red cartoon: holo LasR protein trajectory, green cartoon: apo LasR protein trajectory

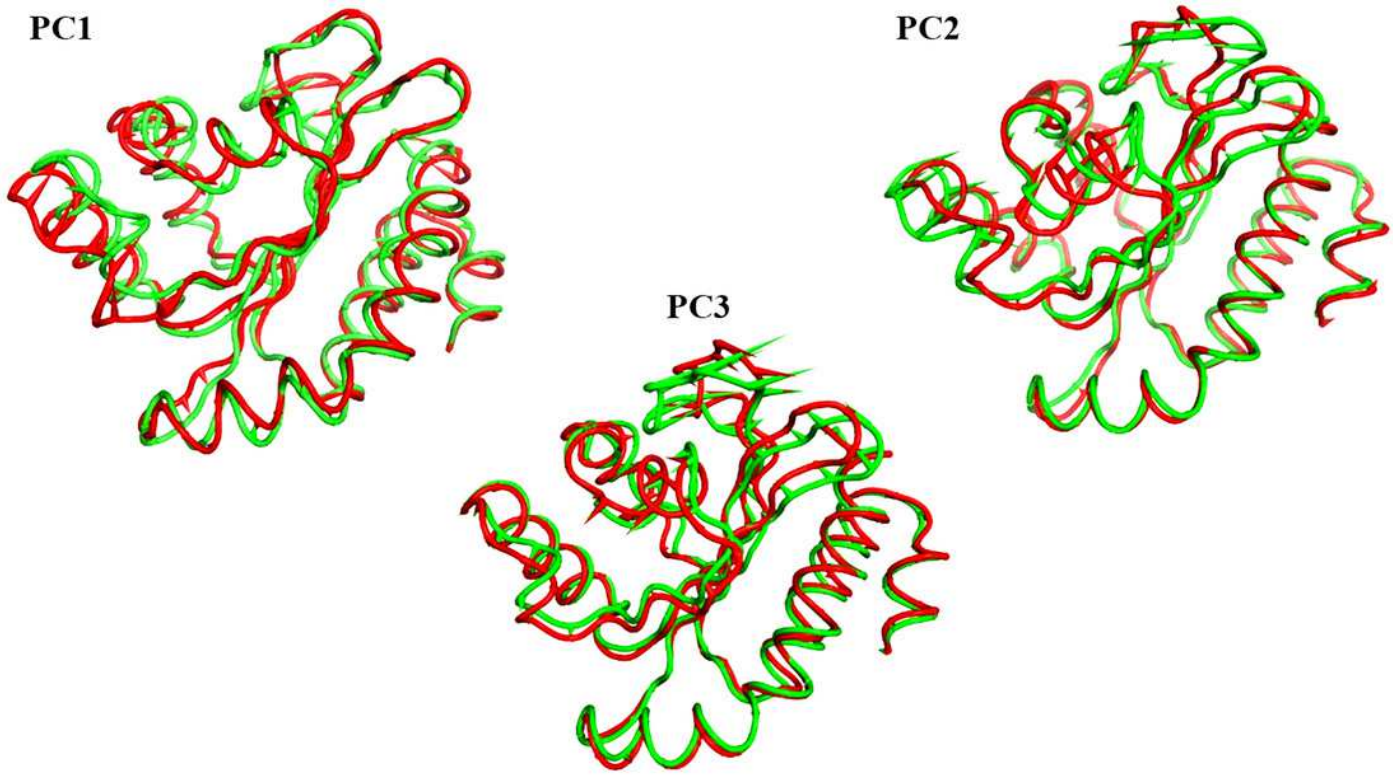

Figure 16

Patuletin's effect at 1/4 MIC against *P. aeruginosa* ability to produce biofilms . Optical density was measured at 570 nm. The data shown represent the means ± standard errors. *P < 0.05

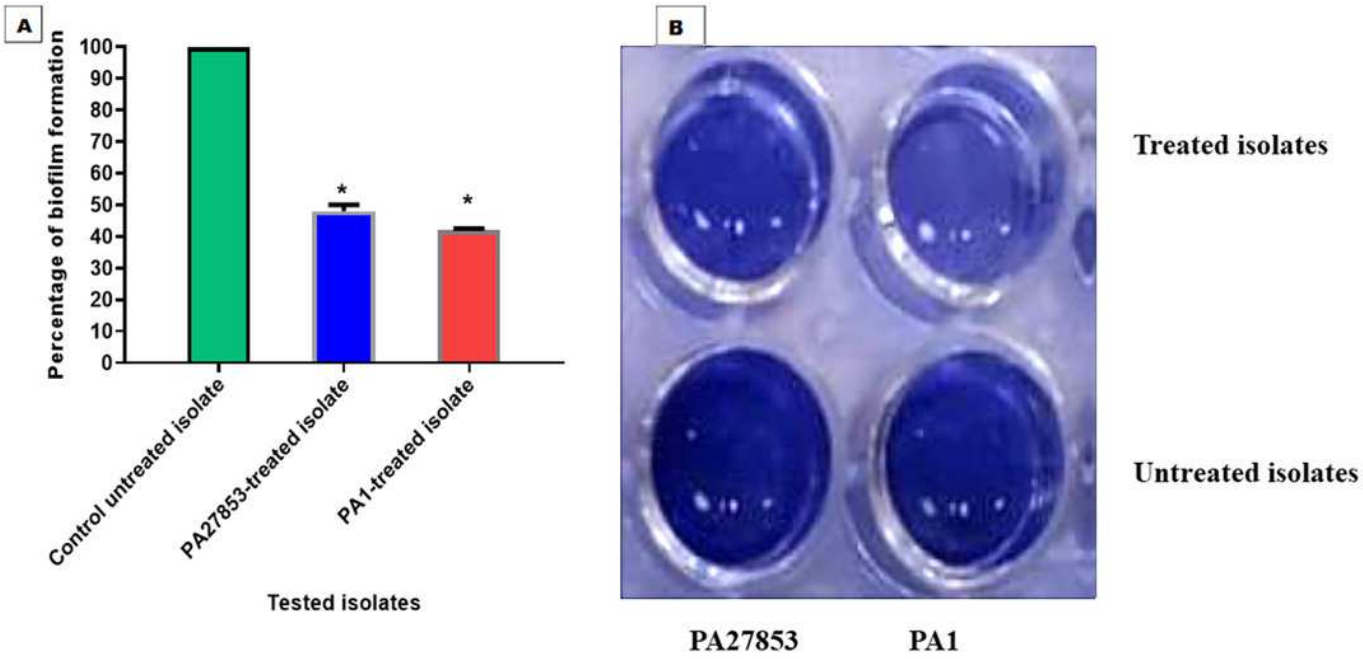

Figure 17

Patuletin at 1/4 MIC significantly reduced the production of pyocyanin in *P. aeruginosa*. The data shown represent the means of three biological experiments ± standard errors. *P < 0.05.

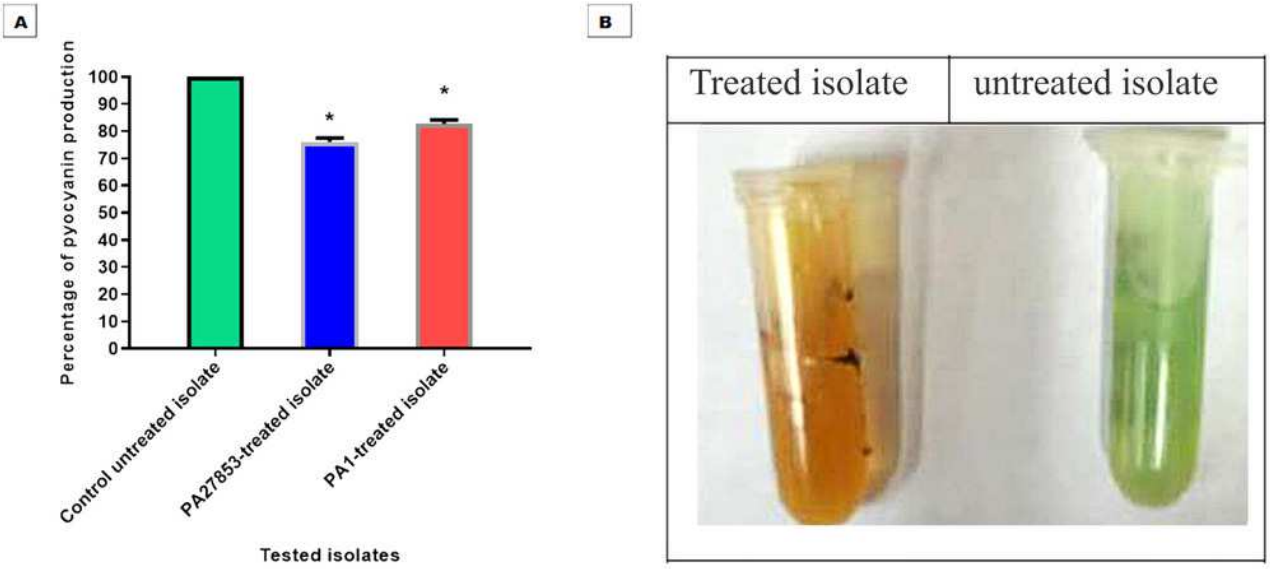

Figure 18

In Patuletin-treated isolates, a significant decrease in proteases activity was observed.

OD_{600} was measured following overnight culturing of bacteria in LB broth with and without 1/4 MIC of Patuletin followed by incubation of supernatants with skim milk for ½ hr at 37 °C. The data shown are the means ± standard errors of three biological experiments with three technical replicates each. *, significant $P < 0.05$

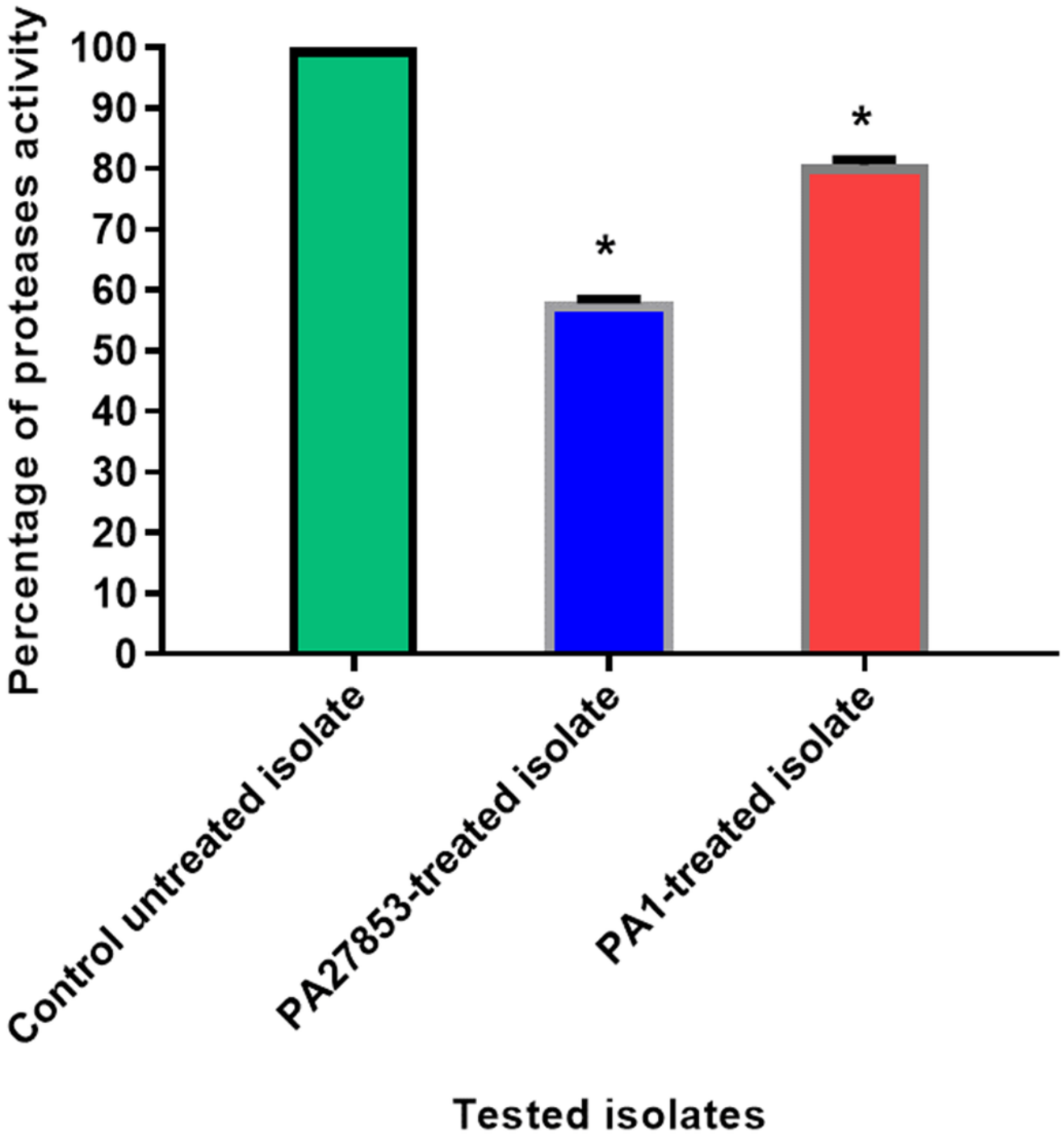
Percentage of proteases activity
100
90
80
70
60
50
40
30
20
10
0
*
*
Control untreated isolate
PA27853-treated isolate
PA1-treated isolate
Tested isolates